Smith, J. V. (1978) Enumeration of 4-connected 3-dimensional nets and classification of frameworks silicates, II. Perpendicular and near-perpendicular linkages from 4.8^2, 3.12^2, and 4.6.12 nets. *American Mineralogist*, **63**, 960–9.

Smith, J. V. (1979) Enumeration of 4-connected 3-dimensional nets and classification of framework silicates, III. Combination of helix, and zigzag, crankshaft and saw chains with simple 2D nets. *American Mineralogist*, **64**, 551–62.

Stewart, R. F. and Spackman, M. A. (1981) Charge density distributions, in *Structure and Bonding in Crystals*, vol. 1, (eds M. O'Keeffe and A. Navrotsky), Academic Press, New York, 279–298.

St. John, J. and Bloch, A. N. (1974) Quantum-defect electronegativity scale for non-transition elements. *Physical Review Letters*, **33**, 1095–8.

Thompson, A. B. (1967) Thermodynamic properties of simple solutions, in *Researches in Geochemistry*, vol. 2, (ed P. H. Abelson) John Wiley, New York, pp. 340–61.

Villars, P. (1983) A three dimensional structural stability diagram for 998 binary AB intermetallic compounds. *Journal of Less-Common Metals*, **92**, 215–38.

Villars, P. (1984a) A three dimensional structural stability diagram for 1011 binary AB_2 intermetallic compounds. *Journal of Less-Common Metals*, **99**, 33–43.

Villars, P. (1984b) Three dimensional structural stability for 648 binary AB_3 and 389 A_3B_5 intermetallic compounds. *Journal of Less-Common Metals*, **102**, 199–211.

Villars, P. (1985) A semiempirical approach to the prediction of compound formation for 3846 binary alloy systems. *Journal of Less-Common Metals*, **109**, 93–115.

Wells, A. F. (1984) *Structural inorganic chemistry*, 5th edn, Oxford University Press, London.

Wood, I. G. and Price, G. D. (1992) A simple, systematic method for the generation of periodic, 2-dimensional, 3-connected nets for the description of zeolite frameworks. *Zeolites*, **112**, 320–327.

Zunger, A. (1980) Systematization of the stable crystal structure of all AB-type binary compounds: a pseudopotential orbital-radii approach. *Physical Review*, **B22**, 5839–72.

Zunger, A. (1981) A pseudopotential viewpoint of the electronic and structural properties of crystals, in *Structure and Bonding in Crystals*, vol. 1, (eds M. O'Keeffe and A. Navrotsky), Academic Press, New York, pp. 49–72.

Zunger, A. and Cohen, M. L. (1979) First-principles non-local pseudopotential approach in the density-functional formalism: II. Application to electronic and structural properties of solids. *Physical Review*, **B20**, 4082–108.

CHAPTER TWO

Bond topology, bond valence and structure stability

Frank C. Hawthorne

2.1 Introduction

There are approximately 3500 known minerals, varying from the simple (native iron) to the complex (mcgovernite has approximately 1200 atoms in its unit cell) and spanning a wide range in bond type, from metallic (native gold) through 'covalent' (pyrite), to 'ionic' (halite). Most of us unconsciously divide the minerals into two groups: *rock-forming* and *other*. The rock-forming minerals are quantitatively dominant but numerically quite minor, whereas the other minerals are the reverse. Although this may seem a rather frivolous basis for such a division, there are actually some fairly important features to it that bear further examination.

First let us look at the rock-forming minerals. Each of these is stable over a wide range of conditions (pressure, temperature, pH, etc.). In response to changing external conditions, some adjust their structural state (degree of cation and/or anion ordering over non-equivalent structural sites), chemical composition, and the geometrical details of their crystal structure; others retain the same state of internal order and bulk chemistry, adjusting just their structural geometry. The common factor that is characteristic of all these minerals is that the topological details of their bond networks do not change very frequently, i.e. the mineral retains its structural integrity over a wide range of temperature, pressure, and component activities. By and large, the basic bond networks of these structures tend to be quite simple, and we usually follow changes in conditions of equilibration via changes in structural state and/or bulk composition.

Similar considerations for the *other* minerals lead to a totally different set of generalizations. Each of these minerals tends to be stable over a very limited range. In response to changing external conditions, these minerals usually break down and form new phases. Thus, the topological characteristics of the bond networks change very rapidly, and this is complicated by the fact that these structures tend to be very complex. Further difficulties arise from the widespread and varied structural role of (H_2O), a component that has not been well understood in the past.

The Stability of Minerals. Edited by G. D. Price and N. L. Ross.
Published in 1992 by Chapman & Hall, London. ISBN 0 412 44150 0

Progress in understanding the behaviour of the other group has been hindered in the past by the lack of a standard approach to the problem. With the rock-forming minerals, we know what to do. We make field observations, analyse the minerals to determine their bulk composition, determine their crystal structure and structural state, measure the thermodynamic properties, do phase-equilibria studies; the result is a fairly good understanding of their behaviour in geological processes, and a good basis for developing computational methods for structure–property calculations. With the other minerals, the complexity of the problem (e.g. rocks containing 50 or so minerals in an obviously non-equilibrium association) defies complete analysis along standard lines.

Extensive field observations have shown that there is consistency of mineral occurrence in these complex environments. Systematic work has shown that consistent crystallization/alteration sequences of minerals can be recognized (e.g. see Fisher, 1958, for an analysis of pegmatitic phosphate minerals), but the geochemical thread linking these minerals together was not apparent. The increase in speed and power of crystallographic techniques provided new impetus, and work by Moore (1973; 1982) has shown that general features of phosphate paragenesis are paralleled by structural trends in the constituent minerals. Since then, efforts have been made to generalize these ideas, introduce quantitative arguments and provide some sort of theoretical underpinnings to this approach. Here, we will develop the important basic ideas and show how they may be used to understand the behaviour of structurally complex minerals.

2.2 Structures as graphs

One of the problems with thinking about structures is that our normal representations of a crystal come in two forms:

1. a list of atom coordinates with unit cell and symmetry information; this is the representation used by the physicist;
2. a view of the structure based on assumptions as to which atom is bonded to which; this is the representation of the chemist.

Using representation (1), we can do all sorts of structure–property calculations, provided that we have appropriate potentials and sufficient computing power; the problem with this is that it cannot be used for many complex minerals, and offers little or no intuitive feel for the behaviour of minerals in geological processes. Using representation (2), we can make qualitative arguments *à la* Pauling's rules, but we do not have a quantitative expression of the important features of a structure. It is with these problems in mind that graph theory can help us.

Consider the four atoms shown in Figure 2.1, in which the lines represent

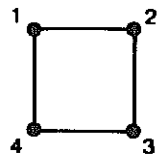

	1	2	3	4
1	–	1	0	1
2	1	–	1	0
3	0	1	–	1
4	1	0	1	–

Graph Adjacency matrix

Figure 2.1 A hypothetical molecule consisting of four atoms (•) joined by chemical bonds (——); as drawn, this is a labelled graph (left). An algebraic representation of this graph is the adjacency matrix (right).

chemical bonds between the atoms. This representation, a series of points joined by a series of lines, is the visual representation of a graph. Formally, we may define a graph as a non-empty set of elements, V(G), called vertices, and a non-empty set of unordered pairs of these vertices, E(G), called edges. If we let the vertices of the graph represent atoms (as in Figure 2.1) or groups of atoms, and the edges of the graph represent chemical bonds (or linkages between groups of atoms), then our graph may represent a molecule.

However, we need some sort of digital representation of this graph, something that we can manipulate algebraically. To do this, we introduce an algebraic representation of the graph in the form of a matrix (Fig. 2.1). Each column and row of the matrix is associated with a specific (labelled) vertex, and the corresponding matrix entries denote whether or not two vertices are adjacent, that is joined by an edge. If the edges of the graph are weighted in some form such that the matrix elements denote this weighting, then this matrix is called the *adjacency matrix*. Thus the adjacency matrix is a digital representation of the graph, which is in turn an analogue representation of the structure. The adjacency matrix does not preserve the geometrical features of the structure; information such as bond angles is lost. However, it does preserve information concerning the *topological* features of the bond network, with the possibility of carrying additional information concerning the strengths (or orders) of chemical bonds. Thus, we have a way of quantifying the topological aspects of the bond network of a molecular group. It remains to determine the significance of this information. To do this, we will now examine some of the connections that have recently developed between contemporary theories of chemical bonding and topological (or graphical) aspects of structure. I shall only sketch the outlines of the molecular orbital arguments, except where they serve to emphasize the equivalence or similarity between energetics of bonding and topological aspects of structure. Excellent reviews are given by Burdett (1980), Hoffman (1988), and Albright *et al.* (1985).

2.3 Topological aspects of molecular orbital theory

2.3.1 Molecules

Molecules are built from atoms, and a reasonable first approach to the electronic structure and properties of molecules is to consider a molecule as the sum of the electronic properties of the constituent atoms, as modified by the interaction between these atoms. The most straightforward way of doing this is to construct the molecular orbital wave function from a *Linear Combination of Atomic Orbitals*, the LCAO method of the chemist and the tight-binding method of the physicist. These molecular orbital wave functions are eigenstates of some (unspecified) effective one-electron Hamiltonian, H^{eff}, that we may write as:

$$H^{\text{eff}}\psi = E\psi \tag{1}$$

where E is the energy (eigenvalue) associated with ψ, and the LCAO molecular orbital wave function is written as

$$\psi = \sum_i c_i \phi_i \tag{2}$$

where $\{\phi_i\}$ are the valence orbitals of the atoms of the molecule, and c_i is the contribution of a particular atomic orbital to a particular molecular orbital.

The total electron energy of the state described by this wave function may be written as

$$E = \frac{\int \psi^* H^{\text{eff}} \psi \, d\tau}{\int \psi^* \psi \, d\tau} = \frac{\langle \psi | H^{\text{eff}} | \psi \rangle}{\langle \psi | \psi \rangle} \tag{3}$$

in which the integration is over all space. Substitution of (2) into (3) gives

$$E = \frac{\sum_i \sum_j c_i c_j \langle \phi_i | H^{\text{eff}} | \phi_j \rangle}{\sum_i \sum_j c_i c_j \langle \phi_i | \phi_j \rangle} \tag{4}$$

This equation may be considerably simplified by various substitutions and approximations:

1. The term $\langle \phi_i | \phi_j \rangle$ is the overlap integral between atomic orbitals on different atoms; we will denote this as S_{ij}, and note that it is always $\leqslant 1$; when $i=j$, $\langle \phi_i | \phi_j \rangle = 1$ for a normalized (atomic) basis set of orbitals.
2. We write $\langle \phi_i | H^{\text{eff}} | \phi_i \rangle = H_{ii}$; this is called the Coulomb integral, and represents the energy of an electron in orbital ϕ_i; it can be approximated by the orbital ionization potential.

3. We write $\langle \phi_i | H^{\text{eff}} | \phi_i \rangle = H_{ij}$; it represents the interaction between orbitals ϕ_i and ϕ_j, and is called the *resonance integral*; it can be approximated by the Wolfsberg–Helmholtz relationship $H_{ij} = KS_{ij}(H_{ii}+H_{jj})/2$ (Gibbs *et al.*, 1972).

The molecular orbital energies are obtained from equation (4) via the variational theorem, minimizing the energy with respect to the coefficients c_i. The most familiar form is the following *secular determinant* equation, the eigenvalues (roots) of which give the molecular orbital energy levels:

$$|H_{ij} - S_{ij}E| = 0 \tag{5}$$

Here we will consider the Hückel approximation (Trinajstic, 1983), as this most simply demonstrates the topological content of this approach. In the Hückel approximation, all H_{ii} values for the pπ orbitals are set equal to α, all H_{ij} are set equal to β, and all $S_{ij}(i \neq j)$ are set equal to zero. As a very simple example, let us consider cyclobutadiene (Fig. 2.2). Writing out the secular determinant equation in full, we get:

$$\begin{vmatrix} \alpha - E & \beta & 0 & \beta \\ \beta & \alpha - E & \beta & 0 \\ 0 & \beta & \alpha - E & \beta \\ \beta & 0 & \beta & \alpha - E \end{vmatrix} = 0 \tag{6}$$

Let us compare the matrix entrics in equation (6) with the cyclobutadiene structure of Figure 2.2. The diagonal terms $(\alpha - E)$ can be thought of as the 'self-interaction' terms; in the absence of any off-diagonal β terms, there are no chemical bonds formed, and the roots of the equation are the energies of the electrons in the atomic orbitals themselves. When chemical bonding occurs,

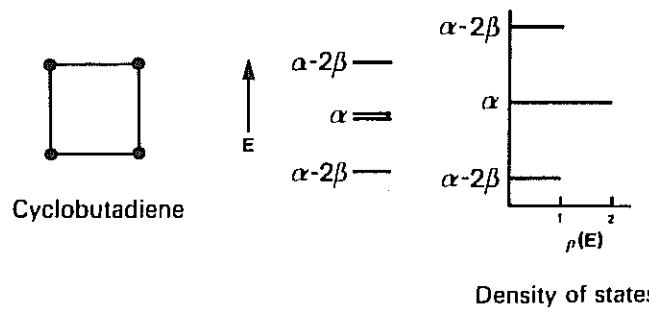

Figure 2.2 The cyclobutadiene molecule (left); to the right are the four roots of equation (6), the electron energy levels expressed in the usual form (centre) and as a density of states form (right).

these energies are modified by the off-diagonal β terms. Thus, when two atoms are bonded together (i.e. atoms 1 and 2 in Figure 2.2), there is non-zero value at this particular (1, 2) entry in the secular determinant; when two atoms are not bonded together (i.e. atoms 1 and 3 in Figure 2.2), then the corresponding determinant entry (1, 3) is zero. Referring back to Figure 2.1, we see that this description is very similar to the adjacency matrix of the corresponding graph. If we use the normalized form of Hückel theory, in which β is taken as the energy unit, and α is taken as the zero-energy reference point (Trinajstic, 1983), then the determinant of equation (6) becomes identical to the corresponding adjacency matrix. The eigenvectors of the adjacency matrix are identical to the Hückel molecular orbitals. Hence it is the *topological (graphical) characteristics* of a molecule, rather than any geometrical details, that determine the form of the Hückel molecular orbitals. For cyclobutadiene, the orbital energies found from the secular determinant (i.e. the four roots of equation (6)) are $E=\alpha+2\beta,\alpha(x2)$, and $\alpha-2\beta$. These are shown in Figure 2.2 both in a conventional energy representation, and as a *density of states* diagram; the latter shows the 'density' of electrons as a function of electron energy.

2.3.2 *Molecular building blocks*

When we consider very complicated problems, we like to resolve them into simple (usually additive) components that are easier to deal with. Molecular and crystal structures are no exception; we recognize structural building blocks, and build hierarchies of structures using these 'molecular bricks'. Let us consider this from a graph theoretic point of view.

A graph G' is a subgraph of a graph G if the vertex- and edge-sets $V(G')$ and $E(G')$ are subsets of the vertex- and edge-sets $V(G)$ and $E(G)$; this is illustrated in Figure 2.3. We may express any graph as the sum of a set of subgraphs. The eigenvalues of each subgraph G' are a subset of the eigenvalues of the main graph G, and the eigenvalues of the main graph are the sum of the eigenvalues of all the subgraphs. In the last section, we saw that the eigenvalues of an adjacency matrix are identical to the Hückel molecular orbitals. Now let us consider the construction of large molecules from smaller building blocks. This provides us with a convenient visual way of analysing the connectivity of our molecule, and of relating molecules together. But this is not all. The fact that the eigenvalues of the graphs of our building blocks are contained in the eigenvalues of the graph of the complete molecule indicates that we may consider our building blocks as *orbital* or *energetic building blocks*. Thus, there is an *energetic basis* for the use of fundamental building blocks in the representation and hierarchical analysis of complex structures.

2.3.3 *Crystals*

So far, we have been considering molecules; however, crystals are far more interesting, particularly if they are minerals. We can envisage constructing a

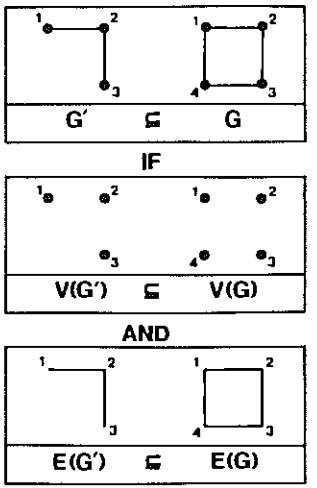

Figure 2.3 The relationship between a graph G and a subgraph G' expressed in terms of the relevant vertex and edge sets.

crystal from constituent molecular building blocks, in this way considering the crystal as a giant molecule. However, it is not clear what influence translational periodicity will have on the energetics of this conceptual building process. Consequently, we will now examine the energetic differences between a molecule and a crystal.

Consider what would happen if we were able to solve the secular determinant equation (6) for a giant molecule; the results are sketched in Figure 2.4. Solution of the secular determinant will give a very large number of molecular orbital energies, and obviously their conventional representation solely as a function of energy is not very useful; such results are more usefully expressed as a density of states diagram (Fig. 2.4), in which the electron occupation of a specific energy interval (band) is expressed as a function of orbital energy.

So what happens in a crystal which has translational symmetry? Obviously, we cannot deal with a crystal using exactly the same sort of calculation, as

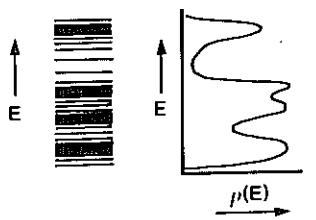

Figure 2.4 The electron energy levels for a giant molecule expressed in the usual way (left) and as a density of states (right).

there are approximately Avogadro's number of atoms in a (macroscopic) crystal, far beyond any foreseeable computational capability. Instead, we must make use of the translational symmetry to reduce the problem to a manageable size. We do this by using what are called Bloch orbitals (Ziman, 1965), in which the orbital content of the unit cell is constrained to the periodicity of the crystal. The secular determinant is solved at a representative set of points within the Brillouin zone (the *special points method*), giving a (hopefully) representative sampling of the orbital energy levels that may be used as the basis of a density of states diagram; this may be smoothed to give the usual density of states diagram. The total orbital energy can then be calculated by integrating the electronic energy density of states up to the Fermi level.

We may summarize the differences between a molecule and a crystal as follows: in a molecule, there is a discrete set of orbital energy levels; in a crystal, these levels are broadened into bands whose occupancies as a function of energy is represented by the corresponding electronic energy density of states.

2.3.4 *The method of moments*

The traditional method for generating the electronic energy density of states has little intuitive connection to what we usually think of as the essential features of a crystal structure, the relative positions of the atoms and the disposition of the chemical bonds. In this regard, Burdett *et al.* (1984) have come up with a very important method of deriving the electronic energy density of states using the method of moments. Here, I will give a brief outline of the method; interested readers should consult the original paper for mathematical details, and are also referred to Burdett (1986; 1987) for a series of applications in solid-state chemistry.

When we solve the secular determinant (equation (6)), we diagonalize the Hamiltonian matrix. The trace of this matrix may be expressed as follows:

$$\mathrm{Tr}(H^n)=\sum_i \sum_{j,k\ldots n} H_{ij}H_{jk}\ldots H_{ni}. \tag{7}$$

A topological (graphical) interpretation of one term in this sum is shown in Figure 2.5. Each H_{ij} term is the interaction integral between orbitals i and j, and hence is equal to β (if the atoms are bonded) or zero (if the atoms are not bonded, or if $i=j$ when $\alpha=0$). Thus a single term $\{H_{ij}H_{ik}\ldots H_{in}\}$ in equation (7) is non-zero only if all H_{ij} terms are non-zero. As the last H_{ij} term is the interaction between the nth orbital and the first orbital, the $\{H_{ij}H_{jk}\ldots H_{ni}\}$ term represents a closed path of length n in the graph of the orbitals (molecule). Thus in Figure 2.5, the term $\{H_{ij}H_{jk}H_{kl}H_{li}\}$ represents the clockwise path of length 4 around the cyclobutadiene pπ orbitals. Thus the complete sum of equation (7) represents all circuits of length n through the graph of the (orbital structure of) the molecule.

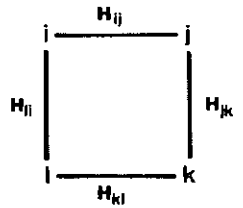

Figure 2.5 Topological interpretation of a single term in the sum of equation 7; for each orbital i, the non-zero terms are a series of circuits of length n with orbital i as the origin; the term shown here has n=4 (for cyclobutadiene).

The trace of the Hückel matrix remains invariant under diagonalization, and thus

$$\mathrm{Tr}(H^n)=\mathrm{Tr}(E^n)=\mu_n \tag{8}$$

where E is the diagonal matrix of eigenvalues (energy levels) and μ_n is the nth *moment* of E, formally denoted by

$$\mu_n=\sum_i E_i^n. \tag{9}$$

The collection of moments $\{\mu_n\}$ may be inverted (see Burdett *et al.*, 1984 for mathematical details) to give the density of states. As we can evaluate $\mathrm{Tr}(H^n)$ directly from the topology of the orbital interactions (bond topology), we thus derive the electronic energy density of states *directly* from the bond topology. Of course, we have already shown that this is the case by demonstrating the equivalence of the secular determinant and the adjacency matrix of the molecule. However, this method of moments generalizes quite readily to infinite systems (i.e. crystals).

For an infinite system, we can define the nth moment of E as

$$\mu_n=\int E^n\rho(E)\,\mathrm{d}E \tag{10}$$

where $\rho(E)$ is the density of states. In principle, the moments may be evaluated as before, and inverted to give the electronic energy density of states. Thus, we see in principle the topological content of the electronic energy density of states in an infinite system, which in turn emphasizes the energetic content of a topological (graphical) representation of (periodic) structure. However, we can go further than this. Burdett (1986) has shown that the energy difference between two structures can be expressed in terms of the first few disparate moments of their respective electronic energy density of states. Thus, when

comparing two structures, the important energetic terms are the most *local topological differences* between the structures. Putting this in structural terms, the important energetic terms involve differences in coordination number and differences in local polyhedral linkage. Furthermore, in structures with bonds of different strengths, each edge of each path (walk) that contributes to each moment will be weighted according to the value of the strength (resonance integral) of the bond defining that edge. Thus, strongly bonded paths through the structure will contribute most to the moments of the electronic energy density of states. The most important energetic features of a structure are thus not only the local connectivity, but the local connectivity of the strongly bonded coordination polyhedra in the structure. This provides an energetic justification for the hypothesis that will be introduced later on, that structures may be ordered according to the polymerization of the more strongly bonded coordination polyhedra (Hawthorne, 1983).

2.4 Topological aspects of crystal chemistry

There are some empirical rules that (sometimes weakly) govern the behaviour of minerals and inorganic crystals, rules that date back to early work on the modern electronic theory of valence and the structure of crystals. The most rigorous rule is that of electroneutrality: *the sum of the formal charges of all the ions in a crystal is zero.* Although we tend to take this rule for granted, it is an extremely powerful constraint on possible chemical variations in crystals. The other rules grew out of observations on a few mineral and inorganic structures. In 1920 the idea was first put forward that atoms have a certain size, and a table of atomic radii was produced; in 1927 the idea of coordination number was introduced, and silicate minerals were considered as polymerizations of coordination polyhedra. These ideas were refined by Pauling (1929; 1960), who systematized them into his well-known rules for the behaviour of 'complex ionic crystals':

1. A coordination polyhedron of anions is formed about each cation, the cation–anion distance being determined by the radius sum, and the ligancy (coordination number) of the cation being determined by the radius ratio.
2. The strength of a bond from a cation to an anion is equal to the cation charge divided by the cation coordination number; in a stable (ionic) structure, the formal valence of each anion is approximately equal to the sum of the incident bond-strengths.
3. The presence of shared faces and edges between coordination polyhedra decreases the stability of a structure; this effect is large for cations of large valence and small ligancy.
4. In a crystal containing different cations, those with large valence and small coordination number tend not to share polyhedral elements with each other.

These rules put some less rigorous constraints on the behaviour of mineral structures, constraints that are traditionally associated with the ionic model of the chemical bond; they allow us to make the following statements about the structure and chemistry of minerals:

1. the formula is electrically neutral;
2. we may make (weak) predictions of likely coordination numbers from the radius ratio rules;
3. we can make fairly good (<0.02 Å) predictions of mean bond lengths in crystals.

Compared with the enormous amount of structural and chemical data available for minerals, our predictive capabilities concerning this information are limited in the extreme. The following questions are pertinent in this regard:

1. Within the constraint of electroneutrality, why do some stoichiometries occur while others do not?
2. Given a specific stoichiometry, what is its bond connectivity (bond topology)?
3. Given a specific stoichiometry and bond connectivity, what controls the site occupancies?
4. What is the role of 'water' of hydration in minerals?

These are some of the basic questions that need answering if we are going to understand the stability of minerals and their role in geological processes from a mechanistic point of view.

2.4.1 Pauling's rules and bond topology

Here I will briefly consider each of Pauling's rules, and indicate how they each relate to the topology of the bond connectivity in structures.

1. The mean interatomic distance in a coordination polyhedron can be determined by the radius sum. This point has been extensively developed up to the present time (Shannon, 1976; Baur, 1987), together with consideration of additional factors that also affect mean bond lengths in crystals (Shannon, 1975). The first rule also states that the coordination number is determined by the radius ratio. This works reasonably well for small high-valence cations, but does not work well for large, low-valence cations. For example, inspection of Shannon's (1976) table of ionic radii shows Na radii listed for coordination numbers from [4] to [12] with oxygen ligands, whereas a radius ratio criterion would indicate that any cation can have (at the most) only two coordination numbers for a specific anion. It is important to note that the coordination number of an atom is one of the lowest moments of the electronic energy density of states.
2. This is also known (rather unfortunately) as the electrostatic valence rule.

It has been further extended by Baur (1970; 1971), who developed a scheme for predicting individual bond lengths in crystals given the bond connectivity, and by Brown and Shannon (1973), who quantitatively related the length of a bond to its strength (bond-valence). The latter scheme has proved a powerful *a posteriori* method of examining crystal structures for crystal chemical purposes. This rule relates strongly to the local connectivity of strong bonds in a structure, and again involves significant low-order moments of the electronic energy density of states.

3.,4. Both of these rules again relate to the local connectivity in a structure, and strongly affect the important low-order moments, both by different short paths resulting from different local bond topologies, and from differences in anion coordination numbers.

The bottom line is that Pauling's rules can all be intuitively related to bond topology and its effect on the low-order moments of the electronic energy density of states.

2.4.2 Ionicity, covalency, and bond topology

Pauling's rules were initially presented as *ad hoc* generalizations, rationalized by qualitative arguments based on an electrostatic model of the chemical bond. This led to an association of these rules with the ionic model, and there has been considerable criticism of the second rule as an 'unrealistic' model for bonding in most solids. Nevertheless, these rules have been too useful to disgard, and in various modifications, continue to be used to the present day. Clearly, their proof is in their applicability to real structures rather than in the details of somewhat vague ionic arguments (Burdett and McLarnan, 1984). In this regard, I will use the terms cation and anion to denote atoms that are of lesser or greater electronegativity, respectively; here, these terms carry no connotation as to models of chemical bonding.

For the past 15 years, Gibbs, Tossell, and coworkers (e.g. Gibbs, 1982; Tossell and Gibbs, 1977) have approached the structure of minerals from a molecular-orbital viewpoint, and have made significant progress in both rationalizing and predicting geometrical aspects of structures. In particular, they have shown that many of the geometrical predictions of Pauling's rules can also be explained by molecular-orbital calculations on small structural fragments. Burdett and McLarnan (1984) show how the same predictions of Pauling's rules can be rationalized in terms of band-structure calculations, again focusing on the covalent interactions, but doing so for an infinite structure. It is interesting to note how these two approaches parallel the arguments given previously concerning the relationship between bond topology and energetics:

1. The energy of a molecular fragment is a function of its graphical/topological characteristics via the form of the secular determinant.
2. The electronic energy density of states of a continuous structure can be

expressed in terms of the sum of the moments of the energy density of states, which is related to the topological properties of its bond network.

The underlying thread that links these ideas together is the topology of the bond network via its effect on the energy of the system. This conclusion also parallels our earlier conclusion that all of Pauling's rules relate to the graphical/topological characteristics of the bond network of a crystal.

We can take this argument a little further. Consider two (dimorphic) structures of the same stoichiometry but different atomic arrangement. As the chemical formulae of the two structures are the same, the atomic components of the energy of each structure must be the same, and the difference in energy between the two structures must relate *completely* to the difference in bond connectivity. This 'general principles' argument emphasizes the importance of bond topology in structural stability, and finds more specific expression in the method of moments developed by Burdett *et al.* (1984). Thus we come to the general conclusion that *arguments of ionicity and/or covalency in structure are secondary to the overriding influence of bond topology on the stability and energetics of structure.*

2.5 Bond-valence theory

From Pauling's second rule and its more quantitative generalization by Brown and Shannon (1973), Brown (1981) has developed a coherent approach to chemical bonding in inorganic structures. Although the empirical bond-valence curves are now widely used, the general ideas of bond-valence theory have not yet seen the use that they deserve. Consequently, I shall review these ideas in detail here, particularly as they can be developed further to deal in a very simple way with the complex hydroxy-hydrated oxysalt minerals.

2.5.1 Bond-valence relationships

According to Pauling's second rule, bond-strength, p, is defined as

$$p = \text{cation valence/cation coordination number} = Z/\text{cn}. \tag{11}$$

If we sum the bond-strengths around the anions, the second rule states that the sum should be approximately equal to the magnitude of the anion valence:

$$\sum_{\text{anion}} p \sim |Z_{\text{anion}}|. \tag{12}$$

Table 2.1 shows the results of this procedure for forsterite and diopside; as is apparent, the rule works well for forsterite but poorly for diopside, with deviations of 0.40 v.u. (valence units ($\sim$20% for the O(2) anion in diopside). Many people have noticed the correlation between deviations from Pauling's

Table 2.1 Pauling bond-strength tables for forsterite and diopside

	Forsterite			
	Mg(1)	Mg(2)	Si	Sum
O(1)	$(\frac{1}{3})^{\times 2}$	$(\frac{1}{3})^{\times 2}$	1	2.00
O(2)	$(\frac{1}{3})^{\times 2}$	$(\frac{1}{3})^{\times 2}$	1	2.00
O(3)	$(\frac{1}{3})^{\times 2}$	$(\frac{1}{3})^{\times 2}$	$1^{\times 2}$	2.00
Sum	2	2	4	
	Diopside			
	Ca	Mg	Si	Sum
O(1)	$(\frac{1}{4})^{\times 2}$	$(\frac{1}{3})^{\times 2}$	1	1.92
O(2)	$(\frac{1}{4})^{\times 2}$	$(\frac{1}{3})^{\times 2}$	1	1.58
O(3)	$(\frac{1}{4})^{\times 2}$		$1^{\times 2}$	2.50
Sum	2	2	4	

second rule and bond-length variations in crystals (see Allmann, 1975), and have parameterized this variation for specific cation–anion bonds. For such schemes, I use the term *bond-valence*, in contrast to the Pauling scheme for which I use the term *bond-strength*; this is merely a convenient nomenclature without any further significance.

The most useful bond-valence–bond-length relationship was introduced by Brown and Shannon (1973). They expressed bond-valence, s, as a function of bond-length, R, in the following way:

$$s = s_0 |R/R_0|^{-N} \tag{13}$$

where s_0, R_0 and N are constants characteristic of each cation–anion pair, and were derived by fitting such equations to a large number of well-refined crystal structures under the constraint that the valence-sum rule work as closely as possible. Values of s_0, R_0 and N are given in Table 2.2. Table 2.3 shows the application of this relationship to the forsterite and diopside structures. Although the valence-sum rule is not obeyed exactly, comparison with Table 2.1 shows great improvement over the simple Pauling bond-strength model.

In equation (13), R_0 is nominally a refined parameter, but is obviously equal to the grand mean bond-length for the particular bond pair and cation coordination number under consideration; also s_0 is equal to the Pauling bond-strength. Thus $(R/R_0) \sim 1$, and s_0 is actually a scaling factor that ensures that the sum of the bond-valences around an atom is approximately equal to the magnitude of its valence.

Table 2.2 Individual bond-valence parameters for some geologically relevant cation–anion pairs

Cation	s_0(v.u.)	R_0(Å)	N
H^{+}	0.50	1.184	2.2
Li^{+}	0.25	1.954	3.9
Be^{2+}	0.50	1.639	4.3
B^{3+}	1.00	1.375	3.9
Na^{+}	0.166	2.449	5.6
Mg^{2+}	0.333	2.098	5.0
Al^{3+}	0.50	1.909	5.0
Si^{4+}	1.00	1.625	4.5
P^{5+}	1.25	1.534	3.2
S^{6+}	1.50	1.466	4.0
K^{+}	0.125	2.833	5.0
Ca^{2+}	0.25	2.468	6.0
Sc^{3+}	0.50	2.121	6.0
Ti^{4+}	0.666	1.952	4.0
V^{5+}	1.25	1.714	5.1
Cr^{6+}	1.50	1.648	4.9
Mn^{2+}	0.333	2.186	5.5
Fe^{3+}	0.50	2.012	5.3
Fe^{2+}	0.333	2.155	5.5
Co^{2+}	0.333	2.118	5.0
Cu^{2+}	0.333	2.084	5.3
Zn^{2+}	0.50	1.947	5.0
Ga^{3+}	0.75	1.837	4.8
Ge^{4+}	1.0	1.750	5.4
As^{5+}	1.25	1.681	4.1

Table 2.3 Bond-valence tables for forsterite and diopside

	Forsterite			
	Mg(1)	Mg(2)	Si	Sum
O(1)	$0.341^{\times 2}$	$0.289^{\times 2}$	1.019	1.938
O(2)	$0.348^{\times 2}$	$0.370^{\times 2}$	0.954	2.042
O(3)	$0.302^{\times 2}$	0.266 0.356	$0.917^{\times 2}$	1.895
Sum	1.982	1.940	3.915	
	Diopside			
	Ca	Mg	Si	Sum
O(1)	$0.316^{\times 2}$	$0.318^{\times 2}$ $0.359^{\times 2}$	1.055	2.048
O(2)	$0.329^{\times 2}$	$0.365^{\times 2}$	1.092	1.786
O(3)	$0.205^{\times 2}$ $0.234^{\times 2}$		0.845	2.245
Sum	2.168	2.084	3.953	

Let us suppose that there is a delocalization of charge into the bonds, together with a reduction in the charge on each atom. For an A–B bond, let the residual charges change by $Z_A p_A$ and $Z_B p_B$ respectively. The (Pauling) bond-strength [=scaling constant s_0 in equation (13)] is given by $Z_A p_A/cn$, where cn is the coordination number of atom A. Inserting these values into equation (13) and summing over the bonds around B gives:

$$\sum_B = p_A \sum s_0 |R/R_0|^{-N} = p_B |Z_B|. \tag{14}$$

If $p_A \sim p_B$, these terms cancel and the bond-valence equation works, provided the relative delocalization of charge from each formally ionized atom is not radically different. Thus the bond-valence equation will apply from 'very ionic' to 'very covalent' situations.

Brown and Shannon (1973) also introduce what they call *universal curves* for bond-valence relationships. These are parameterized such that a single curve applies to all the atoms of an isoelectronic series in the periodic table, and are of the form

$$s = |R/R_1|^{-n}. \tag{15}$$

The constants R_1 and n are given in Table 2.4, and the curves are illustrated in Figure 2.6. These work as well as the individual curves of equation (13), and are often more convenient to use as it is not necessary to distinguish between cations of the same isoelectronic series (e.g. Si and Al, or Mg and Al). A new form of the bond-valence relationship is also given by Brown (1981), but this does not affect the basic ideas of the theory itself.

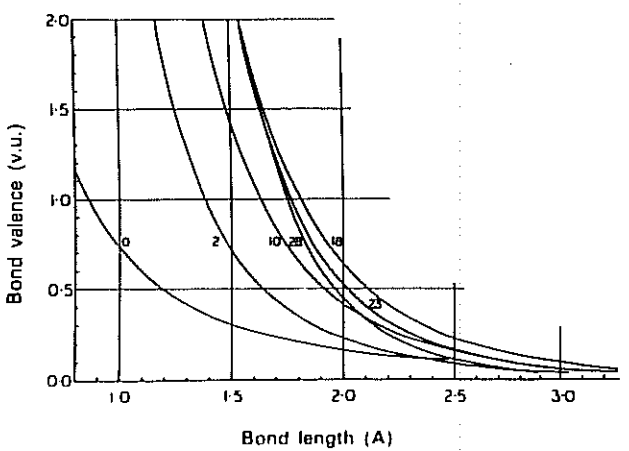

Figure 2.6 Universal bond-valence curves (Brown and Shannon, 1973).

Table 2.4 Universal bond-valence curves for isoelectronic series

Cations	# of core electrons	R_1(Å)	N_1
H^+	0	0.86	2.17
$Li^+Be^{2+}B^{3+}$	2	1.378	4.065
$Na^+Mg^{2+}Al^{3+}Si^{4+}P^{5+}S^{6+}$	10	1.622	4.290
$K^+Ca^{2+}Sc^{3+}Ti^{4+}V^{5+}Cr^{6+}$	18	1.799	4.483
$Mn^{2+}Fe^{3+}$	23	1.760	5.117
$Zn^{2+}Ga^{3+}Ge^{4+}As^{5+}$	28	1.746	6.050

2.5.2 *The conceptual basis of bond-valence theory*

We start by defining a crystal, liquid, or molecule as a network of atoms connected by chemical bonds. For the materials in which we are interested (i.e. minerals), any path through this network contains alternating cations and anions, and the total network is subject to the *law of electroneutrality*: the total valence of the cations is equal to the total valence of the anions. A bond-valence can be assigned to each bond such that the *valence sum rule* is obeyed: *the sum of the bond-valences at each atom is equal to the magnitude of the atomic valence*. If the interatomic distances are known, then the bond-valences can be calculated from the curves of Brown (1981); if the interatomic distances are not known, then the bond-valences can be approximated by the Pauling bond-strengths.

This far, we are dealing just with formalizations from and extensions of Pauling's rules. Although these ideas are important, they essentially involve *a posteriori* analysis: the structure must be known in detail before we can apply these ideas. This is obviously not satisfactory. We need an *a priori* approach to structure stability if we are to develop any predictive capability. In this regard, Brown (1981) introduced a very important idea that abstracts the basic ideas of bond-valence theory, and associates the resulting quantitative parameters with *ions* rather than with bonds (between specific atom pairs). This means that we can examine what would happen if atoms were to bond together in a specific configuration.

If we examine the bond-valences around a specific cation in a wide range of crystal structures, we find that the values lie within ~20% of the mean value; this mean value is thus characteristic of that particular cation. If the cation only occurs in one type of coordination, then the mean bond-valence for that cation will be equal to the Pauling bond-strength; thus P (phosphorus) always occurs in tetrahedral coordination in minerals, and will hence have a mean bond-valence of 1.25 v.u. (Table 2.2). If the cation occurs in more than one coordination number, then the mean bond-valence will be equal to the weighted mean of the bond-valences in all the observed structures. Thus Fe^{2+}

occurs in various coordinations from [4] to [8]; the tendency is for [4] and [5] to be more common than [7] and [8], and hence the mean bond-valence is 0.40 v.u. As the mean bond-valence correlates with formal charge and cation size, then it should vary systematically through the periodic table; this is in fact the case. Table 2.5 shows these characteristic values, smoothed across the periods and down the groups of the periodic table.

The mean bond-valence of a cation correlates quite well with the *electronegativity*, as shown in Figure 2.7. Conceptually this is not surprising. The electronegativity is a measure of the electrophilic strength (electron-accepting capacity) of the cation, and the correlation with the characteristic bond-valence (Fig. 2.7) indicates that the latter is a measure of the *Lewis acid strength* of the cation. Thus we have the following definition (Brown, 1981):

The Lewis acid strength of a cation = characteristic (bond-)valence
= atomic (formal)valence/mean coordination number

We can define the Lewis base strength of an anion in exactly the same way—as the characteristic valence of the bonds formed by the anion. However, it is notable that the bond-valence variations around anions are much greater than those around cations. For example, the valences of the bonds to O^{2-} vary between nearly zero and 2.0 v.u.; thus in sodium alum $(Na[Al(SO_4)_2(H_2O)_6]\ (H_2O)_6$, Cromer *et al.*, 1967), Na is in [12]-coordination, and the oxygen to which it is bonded receives 0.08 v.u. from the Na–O bond; conversely in CrO_3 (a pyroxene-like structure without any [6]-coordinated cations), one oxygen is bonded only to Cr^{6+} and receives 2.00 v.u. from the Cr–O bond. With this kind of variation, it is not particularly useful to define a Lewis base strength for a simple anion such as O^{2-}. However, the situation is entirely different if we consider *complex oxyanions*. Consider the

Table 2.5 Lewis acid strengths (vu) for cations

Li	0.22	Sc	0.50	Cu^{2+}	0.45
Be	0.50	Ti^{3+}	0.50	Zn	0.36
B	0.88	Ti^{4+}	0.75	Ga	0.50
C	1.30	V^{3+}	0.50	Ge	0.75
N	1.75	V^{5+}	1.20	As	1.02
Na	0.16	Cr^{3+}	0.50	Se	1.30
Mg	0.36	Cr^{6+}	1.50	Rb	0.10
Al	0.63	Mn^{2+}	0.36	Sr	0.24
Si	0.95	Mn^{3+}	0.50	Sn	0.66
P	1.30	Mn^{4+}	0.67	Sb	0.86
S	1.65	Fe^{2+}	0.36	Te	1.06
Cl	2.00	Fe^{3+}	0.50	Cs	0.08
K	0.13	Co^{2+}	0.40	Ba	0.20
Ca	0.29	Ni^{2+}	0.50	Pb^{2+}	0.20

Values taken from Brown (1981), except Pb^{2+} which was estimated from several oxysalt mineral structures.

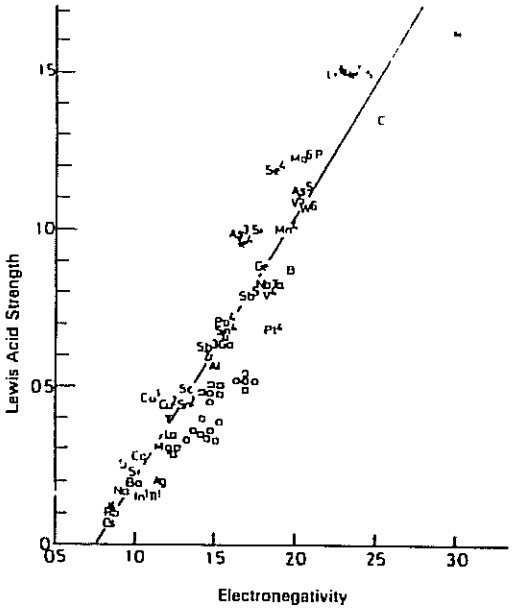

Figure 2.7 Lewis acid strength (mean bond-valence for a specific cation) ns a function of cation electronegativity (Brown, 1981).

$(SO_4)^{2-}$ oxyanion shown in Figure 2.8. Each oxygen receives 1.5 v.u. from the central S^{6+} cation, and hence each oxygen of the group needs an additional 0.5 v.u. to be supplied by additional cations. If the oxygen coordination number is [n], then the average valence of the bonds to O^{2-} (exclusive of the S–O bond) is $0.5/(n-1)$ v.u., thus if $n=2, 3, 4$, or 5, then the mean bond-

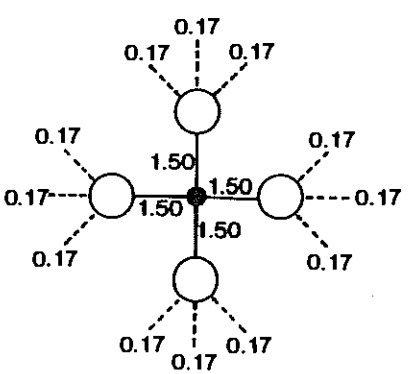

Figure 2.8 Bond-valence structure of the $(SO_4)^{2-}$ oxyanion, with the individual bond-valences shown in vu; • = sulphur, 0 = oxygen.

valencies to the oxygen are 0.50, 0.25, 0.17, or 0.11 v.u., respectively. As all of the oxygens in the $(SO_4)^{2-}$ oxyanion have the same environment, then the average bond-valence received by the oxyanion is the same as the average bond-valence received by the individual oxygens. In this way, we can define the Lewis basicity of an oxyanion. Note that for the $(SO_4)^{2-}$ oxyanion discussed above, the possible average bond-valences are quite tightly constrained (0.50–0.11 v.u.), and we can easily calculate a useful Lewis basicity. Table 2.6 lists Lewis basicities for geologically relevant oxyanions.

These definitions of Lewis acid and base strengths lead to a specific criterion for chemical bonding, the *valence-matching principle*:

The most stable structures will form when the Lewis acid strength of the cation closely matches the Lewis base strength of the anion. We can consider this as the chemical analogue of the handshaking principle in combinatorial mathematics, and the 'kissing' principle in social relationships. As a chemical bond contains two ends, then the ends must match up for a stable configuration to form.

2.5.3 *Simple applications of the valence-matching principle*

Thenardite (Na_2SO_4 (Hawthorne and Ferguson, 1975a)) illustrates both the utility of defining a Lewis base-strength for an oxyanion, and the working of the valence-matching principle (Fig. 2.8). As outlined above, the bond-valences to O^{2-} vary between 0.17 and 1.50 v.u. Assuming a mean oxygen coordination number of [4], the Lewis base strength of the $(SO_4)^{2-}$ oxyanion is 0.17 v.u., which matches up very well with the Lewis acidity of 0.16 v.u. for Na given in Table 2.5. Thus the Na–(SO_4) bond accords with the valence-matching principle, and thenardite is a stable mineral.

Let us consider the compound Na_4SiO_4. The Lewis basicity of the $(SiO_4)^{4-}$ oxyanion is 0.33 v.u. (Table 2.6); the Lewis acidity of Na is 0.16 v.u. These values do not match up, and thus a stable bond cannot form; consequently Na_4SiO_4 is not a stable mineral.

Let us consider Ca_2SiO_4. The Lewis basicity of $(SiO_4)^{2-}$ is 0.33 v.u. and the Lewis acidity of Ca is 0.29 v.u.; these values match up reasonably well, and Ca_2SiO_4 is the mineral larnite.

Consider $CaSO_4$. The relevant Lewis basicity and acidity are 0.17 and

Table 2.6 Lewis basicities for oxyanions of geological interest

$(BO_3)^{3-}$	0.33	$(CO_3)^{2-}$	0.25
$(SiO_4)^{4-}$	0.33	$(NO_3)^{3-}$	0.12
$(AlO_4)^{3-}$	0.42	$(VO_4)^{3-}$	0.25
$(PO_4)^{3-}$	0.25	$(SO_4)^{2-}$	0.17
$(AsO_4)^{3-}$	0.25	$(CrO_4)^{2-}$	0.17

0.29 v.u., respectively; thus according to the valence-matching principle, we do not expect a stable structure to form. However, the mineral anhydrite is stable, the cation and anion coordination numbers both reducing to allow the structure to satisfy the valence-sum rule (Hawthorne and Ferguson, 1975b). However, anhydrite is not very stable, as it hydrates in the presence of water to produce gypsum, $CaSO_4.2H_2O$; this instability (and as we will show later, the hydration mechanism) is suggested by the violation of the valence-matching principle as considered with Lewis acidity/basicity parameters.

Thus we see the power of the valence-matching principle as a simple way in which we can consider the possibility of cation–anion interactions of interest. It is important to recognize that this is an *a priori* analysis, rather than the *a posteriori* analysis of Pauling's second rule and its various modifications.

2.5.4 *Bond-valence theory as a molecular orbital model*

As noted above, there has been considerable criticism of Pauling's second rule and its more recent extensions, criticisms based on its perception as a description of ionic bonding. This viewpoint is totally wrong. In their original work, Brown and Shannon (1973) emphasize the difference between bond-valence theory and the ionic model. In bond-valence theory, the structure consists of a series of atomic cores held together by valence electrons that are associated with the chemical bonds between atoms; they also explicitly state that the valence electrons may be associated with chemical bonds in a symmetric (covalent) or asymmetric (ionic) position. However, *a priori* knowledge of the electron distribution is not necessary, as it is quantitatively derived from the application of the bond-valence curves to the observed structure. Indeed, Burdett and Hawthorne (1992) show how the bond-valence bond-length relationship may be derived algebraically from a molecular orbital description of a solid in which there is a significant energy gap between the interacting orbitals on adjacent atoms. *Thus we may consider bond-valence theory as a very simple form of molecular orbital theory, parameterized via interatomic distance rather than electronegativity or ionization potential*, and (arbitrarily) scaled via the valence-sum rule.

2.6 Structural hierarchies

The need to organize crystal structures into hierarchical sequences has long been recognized. Bragg (1930) classified the silicate minerals according to the way in which the (SiO_4) tetrahedra polymerize, and this was developed further by Zoltai (1960) and Liebau (1985). The paragenetic implications of this are immediately apparent by comparing this scheme with Bowen's discontinuous reaction series in a fractionating basaltic magma (Fig. 2.9). This suggests that structure has a major influence on mineral paragenesis. Further developments along similar lines are the classification of the aluminium hexafluoride minerals

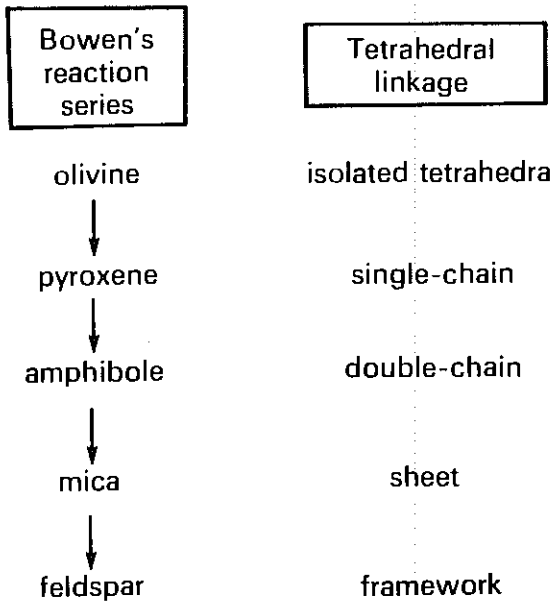

Figure 2.9 Bowen's reaction series shown as a function of the polymerization characteristics of the structures involved.

(Pabst, 1950; Hawthorne, 1984a) and the borate minerals (Christ, 1960; Christ and Clark, 1977), both of which focus on the modes of polymerization of the principal oxyanions. Such an approach to hierarchical organization is of little use in minerals such as the phosphates or the sulphates, in which the principal oxyanion does not self-polymerize. Moore (1984) developed a very successful classification of phosphate minerals, based on the polymerization of divalent and trivalent metal octahedra, and again showed the influence of structure on mineral paragenesis (Moore, 1973). However, all these hierarchical schemes focus on specific chemical classes of minerals. From a paragenetic point of view, this introduces divisions between different chemical classes of minerals, divisions that the natural parageneses indicate to be totally artificial.

2.6.1 *A general hypothesis*

Hawthorne (1983) has proposed the following hypothesis: *structures may be (hierarchically) ordered according to the polymerization of the coordination polyhedra with higher bond-valences.* There are three important points to be

made with regard to this idea:

1. We are defining the structural elements by bond-valences rather than by chemistry; consequently, there is no division of structures into different chemical groups except as occurs naturally via the different 'strengths' of the chemical bonding.
2. We can rationalize this hypothesis from the viewpoint of bond-valence theory. First, let us consider the cations in a structure. The cation bond-valence requirements are satisfied by the formation of anion coordination polyhedra around them. Thus, we can think of the structure as an array of complex anions that polymerize in order to satisfy their (simple) anion bond–valence requirements according to the valence-sum rule. Let the bond-valences in an array of coordination polyhedra be represented by s_0^i $(i=1,n)$ where $s_0^i > s_0^{i+1}$. The valence-sum rule indicates that polymerization can occur when

$$s_0^1 + s_0^i < |V_{anion}| \tag{16}$$

and the valence-sum rule is most easily satisfied when

$$s_0^1 + s_0^i = |V_{anion}| \tag{17}$$

This suggests that the most important polymerizations involve those coordination polyhedra with higher bond-valences, subject to the constraint of equation (16), as these linkages most easily satisfy the valence-sum rule (under the constraint of maximum volume).
3. Earlier we argued that the topology of the bond network is a major feature controlling the energy of a structure. The polymerization of the principal coordination polyhedra is merely another way of expressing the topology of the bond network, and at the intuitive level, we can recognize an energetic basis for the hierarchical organization of structures according to the details of their polyhedral polymerization.

2.6.2 *Structural specifics*

Many classifications of complex structures recognize families of structures based on different arrangements of a *fundamental building block* (FBB). This is a tightly bonded unit within the structure, and can be envisaged as the inorganic analogue of a molecule in an organic structure. The FBB is usually a *homo-* or *heteropolyhedral cluster* of coordination polyhedra that have the strongest bond-valence linkages in the structure. The FBB is repeated, usually polymerized, to form the *structural unit*, a complex anionic polyhedral array whose charge is balanced by the presence of large low-valence *interstitial* cations (usually alkalis or alkaline earths). These definitions are illustrated for the mineral tornebohmite in Figure 2.10. The various structural units can be

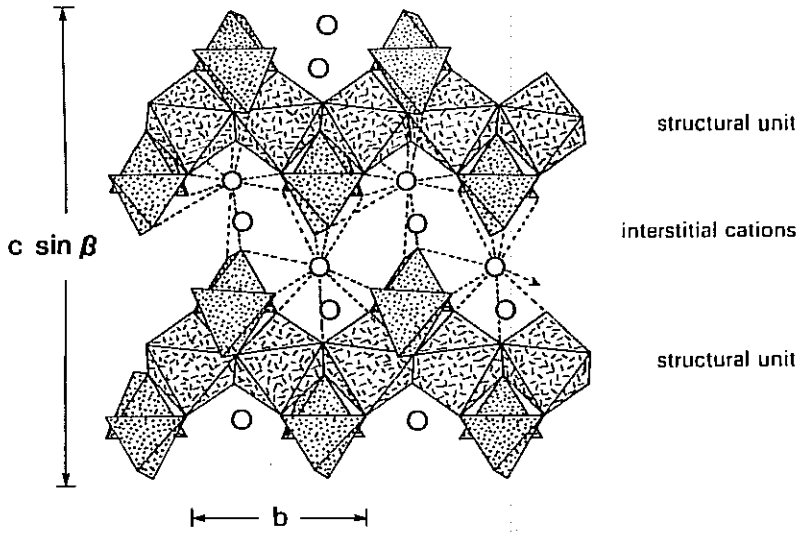

Figure 2.10 The structural unit (as shaded polyhedra) and interstitial cations (as circles) for tornebohmite, $(RE)_2[Al(SiO_4)_2(OH)]$; for clarity, not all bonds from the interstitial cations to the structural unit are shown.

arranged according to the mode of polymerization:

1. unconnected polyhedra
2. finite clusters
3. infinite chains
4. infinite sheets
5. infinite frameworks

Most work has focused on minerals with tetrahedra, triangles, and octahedra as principal components of the structural unit (Hawthorne, 1979; 1984a; 1985a; 1986; 1990; Moore, 1970a, b; 1973; 1974; 1975; 1984), although there has been some notable work (Moore, 1981) on structures with important higher coordinations. Here we will examine minerals based on tetrahedra and octahedra, concentrating specifically on the general stoichiometries $M(T\phi_4)\phi_n$ and $M(T\phi_4)_2\phi_n$ (M = [6]-coordinate, T = [4]-coordinate, ϕ = unspecified anion); these are quantitatively and petrologically most important, as well as showing the most structural diversity.

2.6.3 *Unconnected polyhedra*

Minerals of this class are listed in Table 2.A1 (Appendix p. 77). The tetrahedra and octahedra are linked together by large low-valence interstitial cations and by hydrogen bonding; thus the (H_2O) group plays a major role in the

structural chemistry of this particular class of minerals. The tetrahedral cations are coordinated by oxygens, and the octahedral cations are coordinated predominantly by (H_2O) groups; the exceptions to the latter are khademite and the minerals of the fleischerite group (Table 2.A1), in which the octahedral groups are $(Al(H_2O)_5F)$ and $(Ge(OH)_6)$, respectively. It is notable that khademite is the only $M(T\phi_4)\phi_n$ structure (in this class) with a trivalent octahedral cation; all other minerals have divalent octahedral cations. Similarly, the fleischerite group minerals are the only $M(T\phi_4)_2\phi_n$ minerals (in this class) with tetravalent octahedral cations; all other minerals of this stoichiometry have trivalent octahedral cations.

There is one very notable generalization that comes from an inspection of Table 2.A1. All $M(T\phi_4)_2\phi_n$ structures have interstitial cations, whereas virtually none of the $M(T\phi_4)\phi_n$ structures have interstitial cations. The one exception to this is struvite, $NH_4[Mg(H_2O)_6][PO_4]$, in which the cation is the complex group $(NH_4)^+$ which links the isolated polyhedra together via hydrogen bonds, as is the case for the rest of the $M(T\phi_4)\phi_n$ unconnected polyhedra structures. For the other cases in which the stoichiometry would suggest that an interstitial cation is needed for electroneutrality reasons (e.g. $M^{2+} = Mg$, $T^{5+} = P$, As), we get an acid phosphate or arsenate group instead (e.g. as in phosphorroesslerite and roesslerite, Table 2.A1). Thus for reasons that are as yet unclear, the $M(T\phi_4)\phi_n$ isolated polyhedra structures seemingly will not accept interstitial cations, in contrast to the $M(T\phi_4)_2\phi_n$ structures which always have interstitial cations.

Although this is not the place to go into the details of the hydrogen-bonding schemes in these structures, it should be emphasized that in all structures, the (H_2O) groups participate in an ordered network of hydrogen bonds, and hence are a fixed and essential part of the structure. There has been a tendency in mineralogy to regard (H_2O) as an unimportant component of minerals. Nothing could be further from the truth. Non-occluded (H_2O) is just as important a component as $(SiO_4)^{4-}$ or $(PO_4)^{3-}$ in these minerals, and is the 'glue' that often holds them together.

2.6.4 *Finite cluster structures*

Minerals of this class are given in Table 2.A2 (Appendix). The different types of clusters found in these minerals are illustrated in Figure 2.11.

In jurbanite, the cluster consists of an octahedral edge-sharing dimer of the form $[Al_2(OH)_2(H_2O)_8]$ and an isolated (SO_4) tetrahedron (Figure 2.11(a)). These two fragments are bound together by hydrogen bonding from the octahedral dimer (donor) to the tetrahedron (acceptor), and hence jurbanite is actually transitional between the unconnected polyhedra structures and the finite cluster structures.

In the $M(T\phi_4)\phi_n$ minerals, the structures of the members of the rozenite group are based on the $[M_2(T\phi_4)_2\phi_8]$ cluster (Fig. 2.11(b)), linked solely by

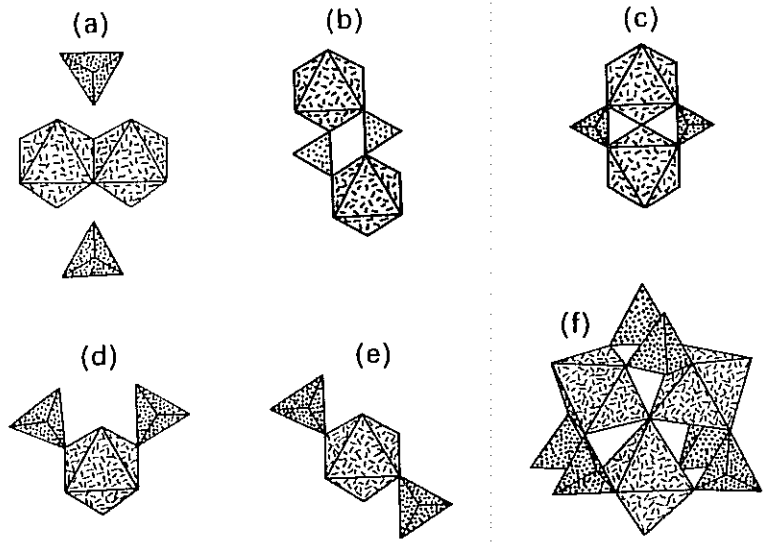

Figure 2.11 Finite polyhedral clusters in $[M(T\phi_4)\phi_n]$ and $[M(T\phi_4)_2\phi_n]$ structures: (a) the $[M_2(T\phi_4)_2\phi_{10}]$ cluster in jurbanite; (b) the $[M_2(T\phi_4)_2\phi_8]$ cluster in the rozenite group minerals; (c) the $[M_2(T\phi_4)_2\phi_7]$ cluster in morinite; (d) the *cis* $[M(T\phi_4)_2\phi_4]$ cluster in roemerite; (e) the *trans* $[M(T\phi_4)_2\phi_4]$ cluster in anapaite, bloedite, leonite, and schertelite; (f) the $[M_3(T\phi_4)_6\phi_4]$ cluster in metavoltine.

hydrogen bonding between adjacent clusters. The morinite structure is based on the $[M_2(T\phi_4)_2\phi_7]$ cluster (Fig. 2.11(c)), linked by interstitial cations as well as inter-unit hydrogen bonds. Hawthorne (1983) derived all possible finite clusters of the form $[M_2(T\phi_4)_2\phi_n]$ with no linkage between tetrahedra and with only corner-sharing between tetrahedra and octahedra. Based on the conjecture that the more stable clusters are those in which the maximum number of anions have their bond-valences most nearly satisfied, four clusters were predicted to be the most stable; two of these are the clusters of Figures 2.11(b),(c).

There is far more structural variety in the $M(T\phi_4)_2\phi_n$ minerals (Table 2.A2). Anapaite, bloedite, leonite and schertelite are based on the simple $[M(T\phi_4)_2\phi_4]$ cluster of Figure 2.11(d), linked by a variety of interstitial cations and hydrogen-bond arrangements. Roemerite is also based on an $[M(T\phi_4)_2\phi_4]$ cluster, but in the *cis* rather than in the *trans* arrangement (Fig. 2.11(e)). Metavoltine is built from a complex but elegant $[M_3(T\phi_4)_6\phi_4]$ cluster (Fig. 2.11(f)) that is also found in a series of synthetic compounds investigated by Scordari (1980, 1981). Again it is notable that the $M(T\phi_4)_2\phi_n$ minerals in this class are characterized by interstitial cations, whereas the bulk of the

$M(T\phi_4)\phi_n$ minerals are not, as was the case for the unconnected polyhedra structures.

The energetic considerations outlined previously suggest that the stability of these finite-cluster structures will be dominated by the topological aspects of their connectivity. Nevertheless, it is apparent from the structures of Table 2.A2 that this is not the only significant aspect of their stability. Figure 2.12 shows the structures of most of the minerals of Table 2.A2. It is very striking that these clusters are packed in essentially the same fashion, irrespective of their nature, and irrespective of their interstitial species. Although a more detailed examination of this point is desirable, its very observation indicates that not only does Nature choose a very small number of fundamental building blocks, but she also is very economical in her ways of linking them together.

2.6.5 *Infinite chain structures*

A large number of possible $[M(T\phi_4)\phi_n]$ and $[M(T\phi_4)_2\phi_n]$ chains can be constructed from fundamental building blocks involving one or two octahedra and one, two or four tetrahedra. Only a few of these possible chains have actually been found in mineral structures, and these are shown in Figure 2.13. Minerals with structures based on these chains are listed in Table 2.A3 (Appendix).

First let us consider the $M(T\phi_4)\phi_n$ minerals, focusing in particular on the first three chains (Figures 2.13(a),(b),(c)). These are the more important of the chains in this group, and it is notable that:

1. they all have a fairly simple connectivity;
2. there is just one particular chain for each type of connectivity between octahedra.

Thus in the first chain, there is no direct linkage between octahedra; in the second chain, there is corner-sharing between octahedra; in the third chain, there is edge-sharing between octahedra.

The more complex chains of Figures 13(d),(e),(f) are found in a smaller number of (far less common) minerals. In addition, there seems to be a trend emerging, that the most complex structural units tend to occur for the ferric iron sulphates.

If we examine the structural units of the $M(T\phi_4)_2\phi_n$ minerals, the same sort of hierarchy is apparent, perhaps even more so than for the $M(T\phi_4)\phi_n$ minerals. Again the three most common and important types of $[M(T\phi_4)_2\phi_n]$ chains are those which show the simplest connectivity. It is significant that they also show the same distribution of connectivities: there is one chain for each of the possible octahedral–octahedral linkages (i.e. no linkage, corner-sharing, and edge-sharing). As indicated in Table 2.A3, these dominate as structural units in the $M(T\phi_4)_2\phi_n$ minerals, with the remaining more complex chains just being found in a few very rare and complicated ferric iron sulphates.

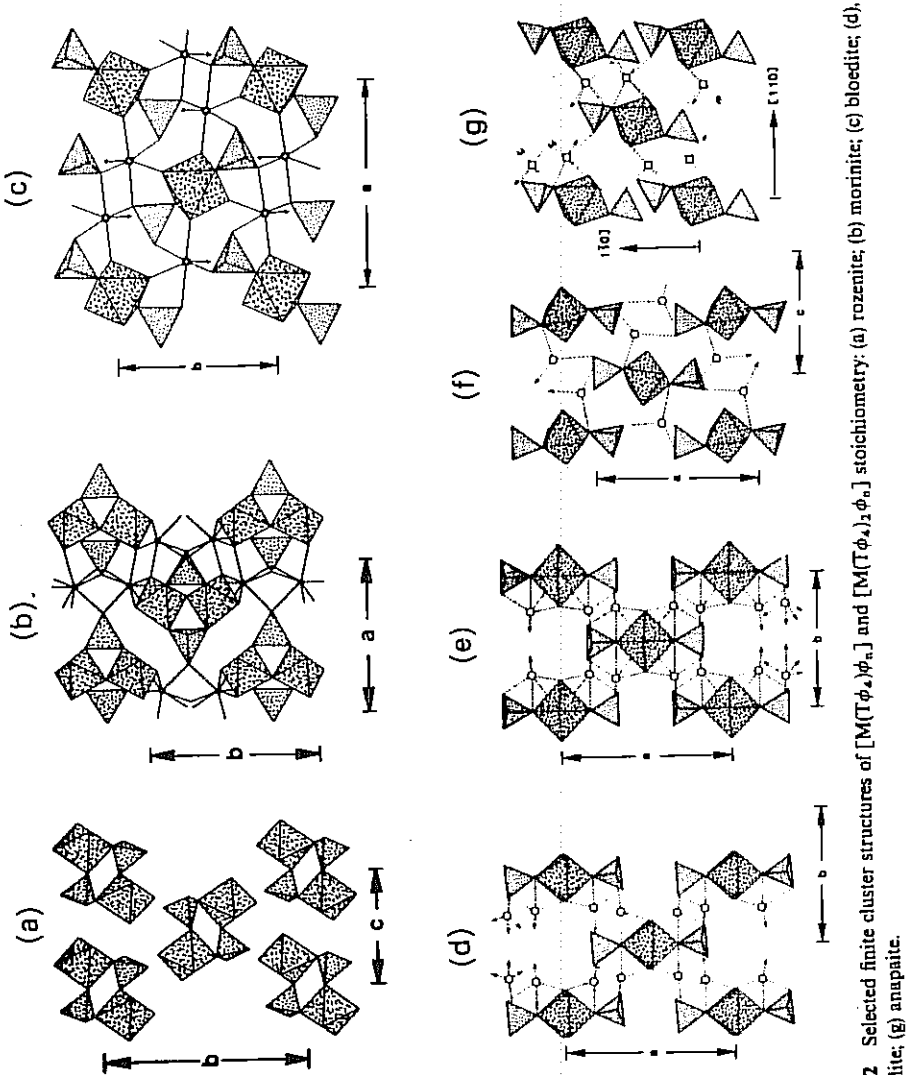

Figure 2.12 Selected finite cluster structures of $[M(T\phi_4)\phi_n]$ and $[M(T\phi_4)_2\phi_n]$ stoichiometry: (a) rozenite; (b) morinite; (c) bloedite; (d), (e) leonite; (f) schertelite; (g) anapaite.

2.6.6 *Infinite sheet structures*

Minerals of this class are given in Table 2.A4 (Appendix). As the degree of polymerization of the structural unit increases, the number of possible bond-connectivities becomes enormous. However, Nature still seems to favour only a fairly small number of them; these are illustrated in Figures 2.14, 2.15, and 2.16.

There is far more variety in the sheet structures of the $M(T\phi_4)\phi_n$ minerals. Notable in the less-connected structural units is that of minyulite (Fig. 14(b)), which is built by condensation (via corner-linkage between octahedra and tetrahedra) of $[M_2(T\phi_4)_2\phi_7]$ clusters that are the structural unit in morinite (Fig. 2.11(c)). The structures of the laueite, stewartite, pseudolaueite, strunzite, and metavauxite groups (Fig. 2.14(c)–(f)) are based on sheets formed from condensation of the vertex-sharing, octahedral–tetrahedral chains of the sort shown in Figures 2.13(b),(h). The tetrahedra cross-link the chains into sheets, and there is much possible variation in this type of linkage; for more details, see Moore (1975). The five structural groups of these minerals are based on the four sheets of Figures 2.14(c)–(f). These sheets are linked through insular divalent-metal octahedra, either by direct corner-linkage to phosphate tetrahedra plus hydrogen bonding, or by hydrogen bonding alone. There is great potential for stereoisomerism in the ligand arrangement of these linking octahedra, but only the *trans* corner-linkages occur in these groups.

More condensed sheets from the $M(T\phi_4)\phi_n$ minerals are shown in Figure 2.15. Again it is notable that we can identify fragments of more primitive (less condensed) structural units in these sheets. In the whitmoreite group sheet (Fig. 2.15a), we can see both the $[M_2(T\phi_4)_2\phi_7]$ cluster of the morinite structure and the $[M(T\phi_4)_2\phi_8]$ cluster of the rozenite group structures (Fig 2.11(c),(b)). Similarly in the $[M(T\phi_4)\phi]$ sheet of the bermanite and tsumcorite structures (Fig. 2.15(b)), we can see the $[M(T\phi_4)\phi_2]$ chain that is the structural unit in the minerals of the linarite group (Fig. 2.13(e)).

The structural sheet units found in the $M(T\phi_4)_2\phi_n$ minerals are shown in Figure 2.16. Again we see this structural building process, whereby our structural units of more primitive connectivities act as fundamental building blocks for the more condensed structural units of corresponding composition. Thus the $[M(T\phi_4)_2\phi_2]$ sheet found in rhomboclase (Fig. 2.16(a)) is constructed from the *cis* $[M(T\phi_4)_2\phi_4]$ cluster that is the structural unit of roemerite (Fig. 12(e)). Similarly, the $[M(T\phi_4)_2\phi_2]$ sheet of olmsteadite (Fig. 2.16(b)) is based on the *trans* $[M(T\phi_4)_2\phi_4]$ cluster (Fig. 2.12(d)) found in anapaite, bloedite, leonite and schertelite. Note that the rhomboclase and olmsteadite sheets are actually *geometrical isomers* (Hawthorne, 1983).

Analogous relationships are obvious for the $[M(T\phi_4)_2]$ merwinite-type sheet and the $[M(T_2\phi_7)\phi_2]$, bafertisite-type sheet (Fig. 2.16(c),(d)). Both are based on the $[M(T\phi_4)_2\phi_2]$ krohnkite chain of Figure 2.13(g), but in each sheet, the chains are cross-linked in a different fashion. In the merwinite sheet,

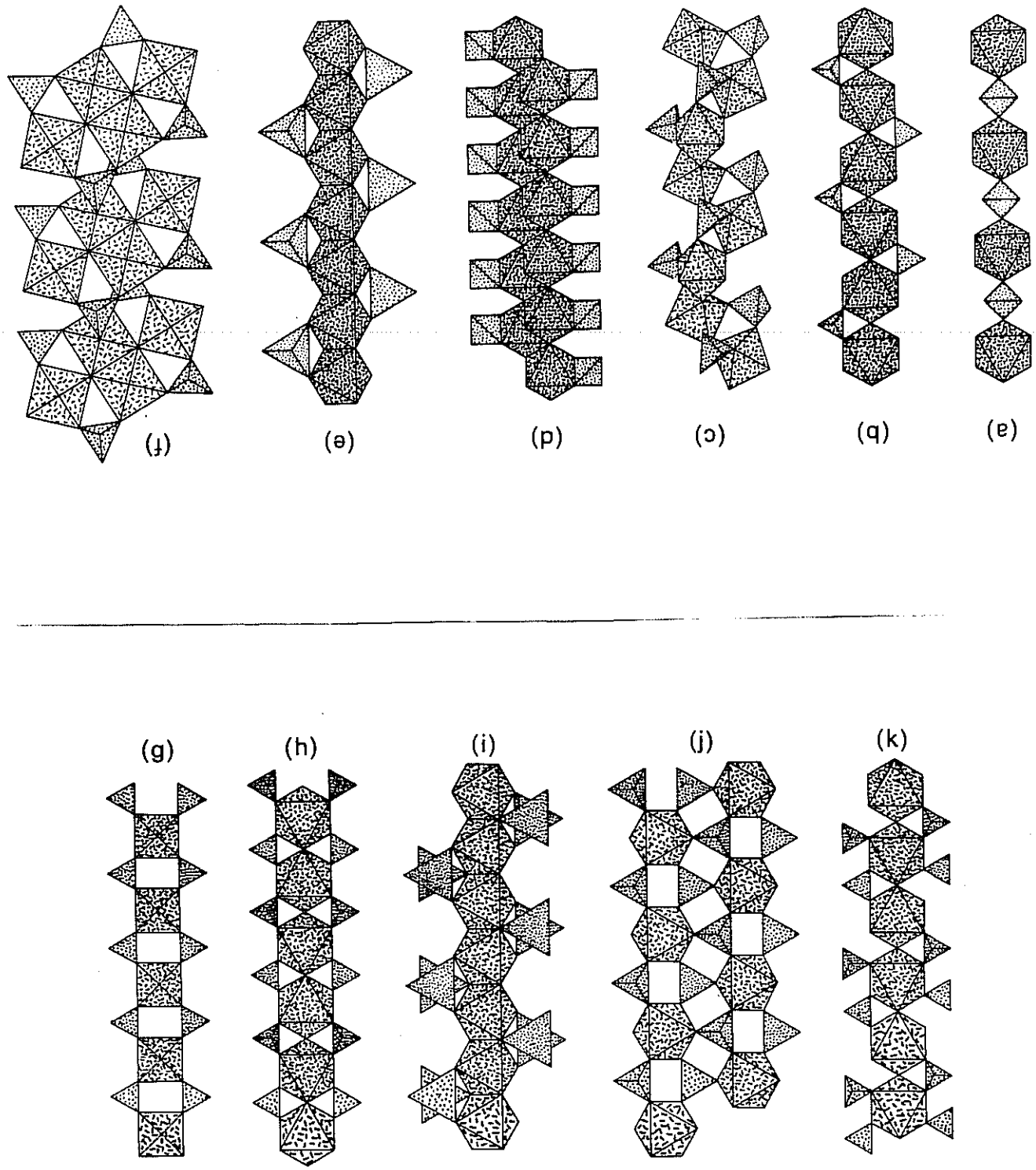

Figure 2.13 Infinite chains in $[M(T\phi_4)\phi_n]$ and $[M(T\phi_4)_2\phi_n]$ structures: (a) the $[M(T\phi_4)\phi_4]$ chain in the chalcanthite group minerals, liroconite and brassite; (b) the $[M(T\phi_4)\phi_3]$ chain found in butlerite, parabutlerite, the childrenite group, and uklonskovite; (c) the $[M(T\phi_4)\phi_3]$ chain in fibbroferrite; (d) the $[M(T\phi_4)\phi]$ chain in chlorotionite; (e) the $[M(T\phi_4)\phi_2]$ chain in the linarite group minerals; (f) the $[M_2(T\phi_4)_4\phi_5]$ chain found in amarantite and hohmannite; (g) the $[M(T\phi_4)_2\phi_2]$ chain in the krohnkite, talmessite, and fairfieldite groups; (h) the $[M(T\phi_4)_2\phi]$ chain found in tancoite, sideronatrite, the jahnsite and segelerite groups, guildite, and yftisite; (i) the $[M(T\phi_4)_2\phi]$ chain found in the brackebuschite, fornacite, and vauquelinite groups; (j) the $[M(T\phi_4)_2\phi]$ chain in ransomite and krausite; (k) the $[M_2(T\phi_4)_4\phi_5]$ chain found in botryogen.

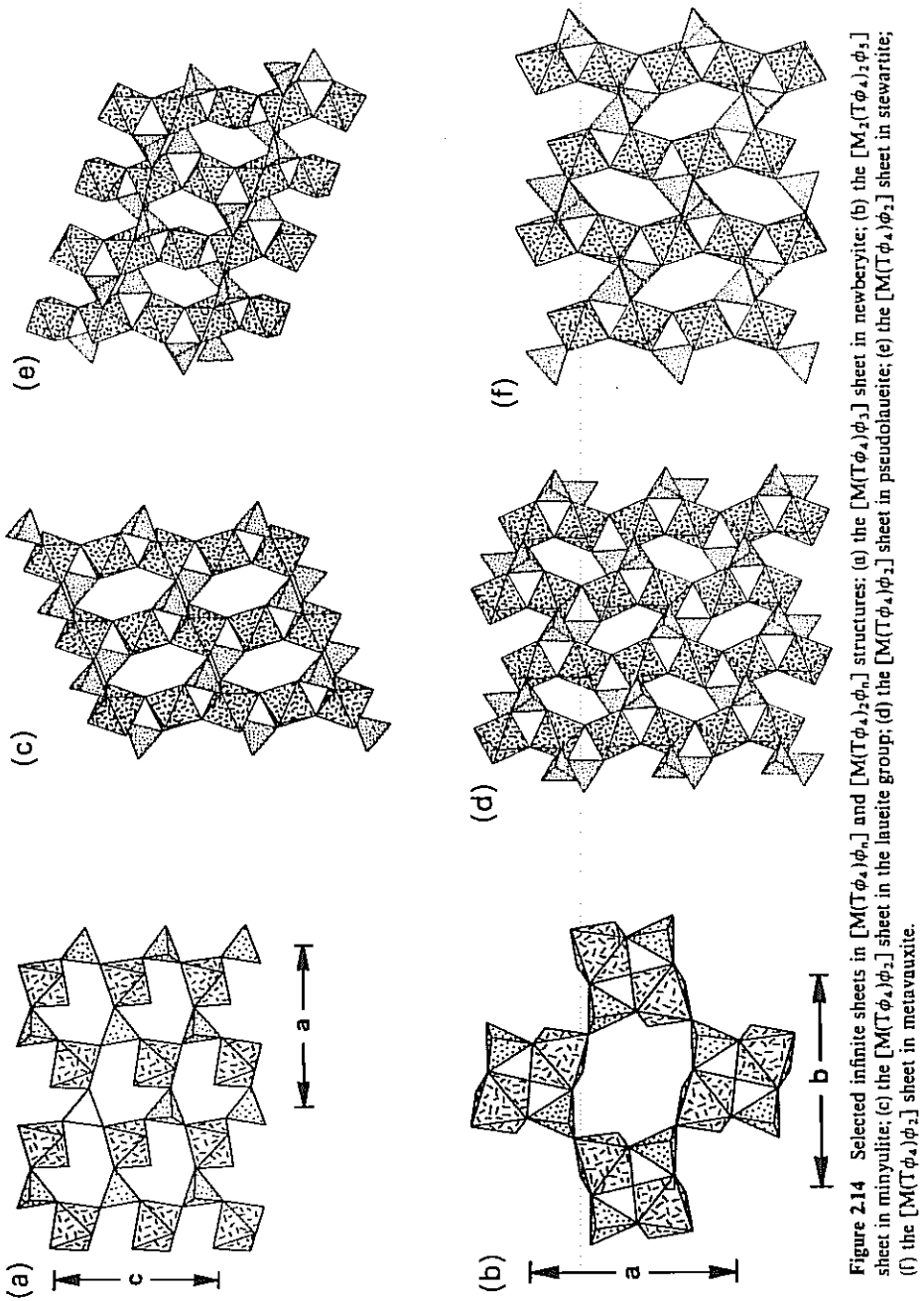

Figure 2.14 Selected infinite sheets in $[M(T\phi_4)\phi_n]$ and $[M(T\phi_4)_2\phi_n]$ structures: (a) the $[M(T\phi_4)\phi_3]$ sheet in minyulite; (c) the $[M(T\phi_4)\phi_2]$ sheet in the laueite group; (d) the $[M(T\phi_4)\phi_2]$ sheet in pseudolaueite; (e) the $[M(T\phi_4)\phi_2]$ sheet in stewartite; (f) the $[M(T\phi_4)\phi_2]$ sheet in metavauxite.

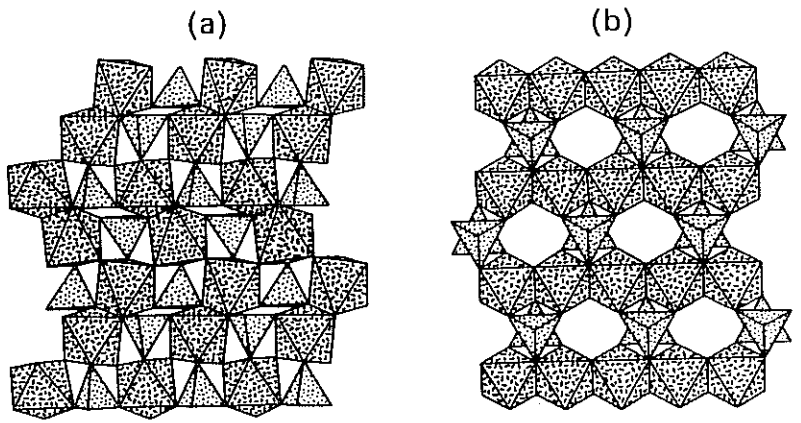

Figure 2.15 Selected infinite sheets in $[M(T\phi_4)\phi_n]$ and $[M(T\phi_4)_2\phi_n]$ structures: (a) the $[M_2(T\phi_4)_2\phi_7]$ sheet in whitmoreite; (b) the $[M(T\phi_4)\phi]$ sheet in tsumcorite and bermanite.

tetrahedra from one chain share corners with octahedra of adjacent chains, with neighbouring tetrahedra pointing in opposite directions relative to the plane of the sheet. In the bafertisite sheet, the $[M(T\phi_4)_2\phi_2]$ chains link by sharing corners between tetrahedra. Thus both sheets are 'built' from the same more primitive structural unit, and these two sheets are in fact *graphical isomers* (Hawthorne, 1983).

2.6.7 *Framework structures*

Minerals of this class are listed in Table A5 (Appendix). Unfortunately, the topological aspects of the framework structures cannot be easily summarized in a graphical fashion, partly because of their number, and partly because of the complexity that results from polymerization in all three spatial dimensions. Consequently, we will consider just a few examples that show particularly clearly the different types of linkages that can occur.

The structure of bonattite is shown in Figure 2.17(a) Now bonattite is quite hydrated (Table 2.A5), and comparison with the minerals of Table 2.A4 suggests that it should be a sheet structure (cf. newberyite, Table 2.A4). Prominent in the structure are the $[M(T\phi_4)\phi_4]$ chains (Fig. 2.13(a)) that also occur as fragments of the newberyite sheet (Fig. 2.14(a)). In bonattite, adjacent chains are skew and link to form a framework; in newberyite, the chains are parallel, and with the same number of interchain linkages, they link to form sheets rather than a framework. Thus bonattite and newberyite are graphical isomers, and provide a good illustration of how different modes of linking the same fundamental building block can lead to structures of very different connectivities and properties.

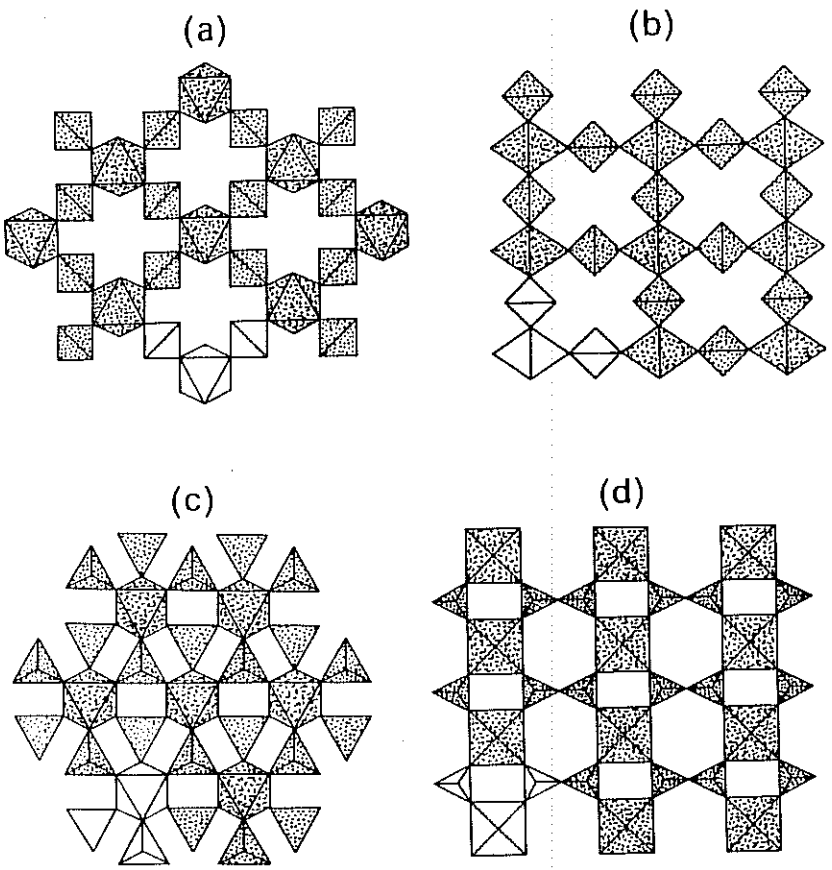

Figure 2.16 Selected infinite sheets in $[M(T\phi_4)\phi_n]$ and $[M(T\phi_4)_2\phi_n]$ structures: (a) the $[M(T\phi_4)_2\phi_2]$ sheet found in rhomboclase; (b) the $[M(T\phi_4)_2\phi_2]$ sheet found in olmsteadite; (c) the $[M(T\phi_4)_2]$ sheet found in the merwinite group and yavapaite; (d) the $[M(T_2\phi_7)\phi_2]$ sheet found in bafertisite.

The structure of titanite is shown in Figure 2.17b; this basic arrangement is found in a considerable number of minerals (Table 2.A5) of widely differing chemistries. The $[M(T\phi_4)\phi]$ framework can be constructed from $[M(T\phi_4)\phi]$ vertex-sharing chains of the sort found in butlerite, parabutlerite, the childrenite group, and uklonskovite (Table 2.A3, Fig. 2.13(b)). The chains pack in a C-centered array and cross-link by sharing corners between octahedra and tetrahedra of adjacent chains. It is notable that this chain is also a fundamental building block of the sheets (Fig. 2.14(c)–(f)) in the laueite, stewartite, pseudolaueite, strunzite, and metavauxite groups (Table 2.A4).

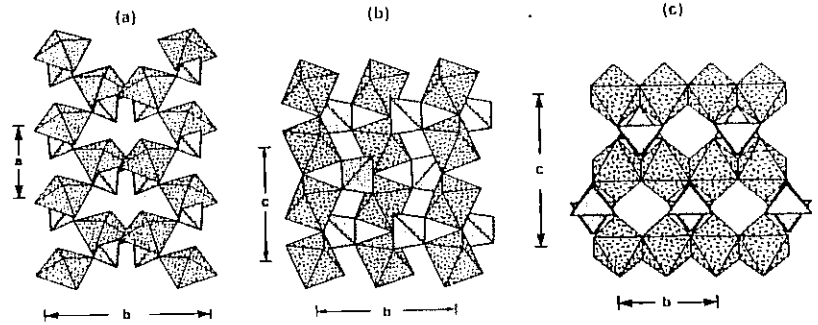

Figure 2.17 Selected framework structures in $[M(T\phi_4)\phi_n]$ and $[M(T\phi_4)_2\phi_n]$ minerals: (a) the $[M(T\phi_4)\phi_3]$ framework structure of bonattite; (b) the $[M(T\phi_4)\phi]$ framework structure of titanite; (c) the $[M(T\phi_4)\phi]$ framework structure of descloizite.

The structure of descloizite is shown in Figure 2.17(c); again this is a popular structural arrangement (Table 2.A5). Prominent features of the tetrahedral–octahedral framework are the edge-sharing chains of octahedra flanked by staggered tetrahedra that link along the chain. This $[M(T\phi_4)\phi]$ chain is found in the structures of the minerals of the linarite group (Figure 2.13(e)), and is also a fundamental building block for the $[M(T\phi_4)\phi]$ sheet (Figure 2.15(b)) that is the structural unit in tsumcorite and bermanite (Table 2.A4).

These three examples show the type of structural variability we find in the framework structures, and also the small number of polyhedral linkage patterns (fundamental building blocks) that occur and seem common to a wide range of structural types. This suggests that these patterns of bond connectivity are very stable, and hence tend to persist from one structure to another. In addition, the incorporation of relatively primitive fragments into more highly condensed structural units tends to support the conceptual approach of considering a large structure both topologically and energetically as an assemblage of smaller structural fragments.

2.7 (OH) and (H_2O) in oxysalt structures

In inorganic minerals, the hydrogen cation H^+ most commonly has a coordination number of [2]; higher coordination numbers are not rare, but for simplicity we will consider the former, as the arguments presented here can easily be generalized to higher coordination numbers. Usually this arrangement undergoes a spontaneous distortion, with the hydrogen ion moving off-centre towards one of the two coordinating anions. The geometry of this arrangement has been very well-characterized by neutron diffraction (Ferraris and Franchini-Angela, 1972); the typical arrangement is shown in Figure 2.18. Brown (1976) has shown that the most common bond-valence distribution is

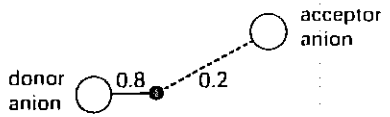

Figure 2.18 Typical geometry of hydrogen coordination: the hydrogen is [2]-coordinated, and spontaneously moves off-centre to form two bonds of the approximate valence shown, and a bent O-H-O angle; the anion closer to the hydrogen is called the 'donor' anion, and the anion further from the hydrogen is called the 'acceptor' anion.

about 0.80 v.u. to the closer oxygen, and approximately 0.20 v.u. to the further oxygen; this generally leads to the stronger bond being subsumed within $(H_2O)^0$ or $(OH)^-$ groups that now become complex anions, and the longer (weaker) bond being referred to as a *hydrogen bond*. The oxygen closer to the hydrogen is called the (hydrogen bond) *donor*, and the oxygen further from the hydrogen is called the (hydrogen bond) *acceptor* (Fig. 2.18).

There are four different hydrogen-bearing groups in minerals: $(OH)^-$, $(H_2O)^0$, $(H_3O)^+$, and $(H_5O_2)^+$; sketches of typical bond-valence distributions for these groups are shown in Figure 2.19. The positively charged groups act as cations and are extremely uncommon, although they have been identified in such minerals as hydronium jarosite ($\{H_3O\}[Fe^{3+}_3(SO_4)_2(OH)_6]$, Ripmeester *et al.*, 1986) and rhomboclase ($\{H_5O_2\}[Fe^{3+}(SO_4)_2(H_2O)_2]$, Mereiter, 1974).

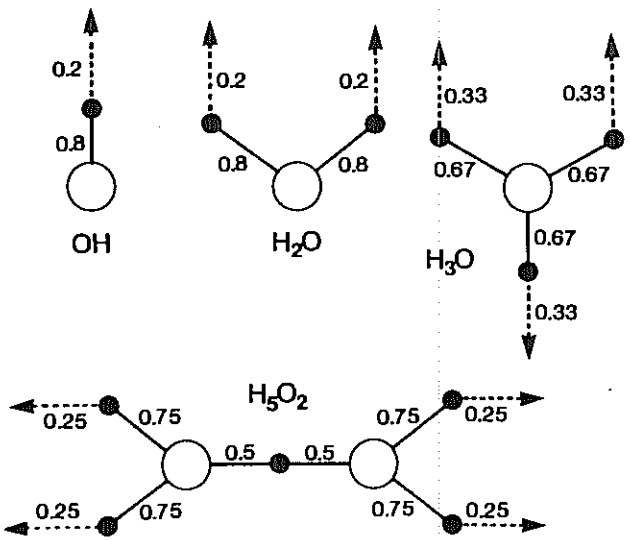

Figure 2.19 Typical bond-valence distributions for the hydrogen-bearing groups found in minerals $(OH)^-$, $(H_2O)^0$, $(H_3O)^+$, and $(H_5O_2)^+$.

On the other hand, the $(OH)^-$ and $(H_2O)^0$ groups play a very important role in the structures of the oxysalt minerals, particularly with regard to the topological properties of their bond networks. The reason for this stems from the extremely directional nature of the bonding associated with these two groups. On the oxygen side of each group, they function as an anion, whereas on the hydrogen side of each group, they function as a cation (Fig. 2.18); it is because of this unusual property that they play such a unique role in the structure and chemistry of minerals.

2.7.1 *(OH) and (H_2O) as components of the structural unit*

The very important role of these groups in the constitution of the structural unit of a mineral stems from their bond-valence distribution (Fig. 2.19). On the anionic side of each group, the bond-valence is relatively strong, approximately 1.2 v.u. for (OH) and 0.4 v.u. for (H_2O); the remainder of the bond-valence requirements of the central oxygen is satisfied by the hydrogens, and on the cationic side of the group, the bond-valence is relatively weak, about 0.2 v.u. for each group (Fig. 2.19). Thus, on the anionic side of the group, the strong bonding constitutes part of the bonding network of the structural unit; conversely, on the cationic side of the group, the hydrogen bond is too weak to form a part of the bonding network of the structural unit. The role of both (OH) and (H_2O) is thus to '*tie off*' the polymerization of the structural unit in specific directions. Consequently, these groups play a crucial role in controlling the class of the polymerization of the structural unit (Hawthorne, 1985a), and hence control many of the physical and chemical properties of a mineral.

An excellent example of this is the structure of newberyite (Sutor, 1967), $[Mg(PO_3OH)(H_2O)_3]$. The structural unit is a sheet of corner-sharing (MgO_6) octahedra and (PO_4) tetrahedra, with the polyhedra arranged at the vertices of a 6_3 net, as illustrated in Figure 2.14(a); the bond-valence structure is shown in Table 2.7. In the (PO_4) tetrahedra, three of the ligands link to (MgO_6) octahedra within the sheet. The other ligand is 'tied off' orthogonal to the sheet

Table 2.7 Bond-valence table for newberyite

	Mg	P	H(6)	H(71)	H(72)	H(81)	H(82)	H(91)	H(92)	Sum
O(3)	0.389	1.399								1.788
O(4)	0.349	1.242	0.20	0.20						1.891
O(5)	0.364	1.232			0.20	0.20				1.996
O(6)		1.095	0.80				0.20			2.095
O(7)	0.326			0.80	0.80			0.20		2.126
O(8)	0.316					0.80	0.80		0.20	2.116
O(9)	0.313							0.80	0.80	1.913
Sum	2.057	4.968	1.0	1.0	1.0	1.0	1.0	1.0	1.0	

by the fact that the oxygen is strongly bonded to a hydrogen atom (i.e. it is a hydroxyl group); the long P–O bond of 1.59 Å contributes a bond-valence of 1.10 v.u. to the oxygen, and the remaining 0.90 v.u. is contributed by the hydrogen atom which then weakly hydrogen-bonds (bond-valence of about 0.10 v.u.) to the neighbouring sheet in the Y-direction. In the (MgO_6) octahedra, three of the ligands link to (PO_4) tetrahedra within the sheets. The other ligands are 'tied off' by the fact that they are (H_2O) groups; the Mg–O bonds of 2.11, 2.12 and 2.13 Å contribute a bond-valence of approximately 0.32 v.u. to each oxygen, and the remaining 1.68 v.u. is contributed by the two hydrogen atoms which then weakly hydrogen-bond (bond-valences of about 0.16 v.u. for each bond) to the neighbouring sheets in the Y direction. The chemical formula of the structural unit is also the chemical formula of the mineral, and the sheet-like nature of the structural unit is controlled by the number and distribution of the hydrogen atoms in the structure.

In newberyite, all intra-unit linkage was stopped at the (OH) and (H_2O) groups. This is not necessarily the case; for specific topologies, both (OH) and (H_2O) can allow intra-unit linkage in some directions and prevent it in others. A good example of this is the mineral artinite (Akao and Awai, 1977), [$Mg_2(CO_3)(OH)_2(H_2O)_3$], the structure of which is shown in Figure 2.20; the bond-valence structure is shown in Table 2.8. The structural unit is a ribbon (chain) of edge-sharing (MgO_6) octahedra, flanked by (CO_3) triangles linked to alternate outer octahedral vertices of the ribbon, and occurring in a staggered arrangement on either side of the ribbon. The anions bonded to Mg and running down the centre of the ribbon are bonded to three Mg cations; they receive about $0.36 \times 3 = 1.08$ v.u. from the Mg cations, and thus receive 0.92 v.u. from their associated hydrogen atoms which then weakly hydrogen-bond (bond-valence approximately 0.08 v.u.) to an adjacent ribbon. The $(OH)^-$ group thus allows linkage in the X and Y directions but prevents linkage in the Z direction.

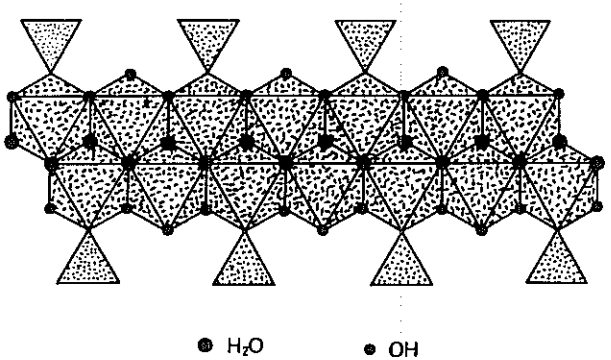

Figure 2.20 The structural unit in artinite, a ribbon of (MgO_6) octahedra and (CO_3) triangles; all simple anions not bonded to carbon are either (OH) or (H_2O).

Table 2.8 Bond-valence table for artinite

	Mg	C	H(1)	H(2)	H(3)	H(4)	Sum
*O(1)	0.391		0.08			0.80 ×2	2.071
*O(1)'	0.391	1.678	0.08				2.149
O(2)		1.264 ×2		0.30	0.30		1.864
OH	0.372 ×2 0.350		0.92				2.018
OW	0.283 ×2			0.70	0.70		1.966
	2.051	4.206	1.00	1.00	1.00	1.00	

*O(1) and O(1)' are disordered, and are both half-occupied.

The anions bonded to Mg and running along the edge of the ribbon are bonded to either one Mg, two Mg, or one Mg and one C, with bond-valence conributions of about 0.3, 0.6, and 1.7 v.u., respectively. The former two ligands are therefore (H_2O) groups which hydrogen bond fairly strongly to anions in the same structural unit and in adjacent structural units. Thus the (H_2O) group bonded to one Mg prevents further unit polymerization in all three directions, whereas the (H_2O) group bonded to two Mg atoms allows polymerization in the Y direction but prevents polymerization in the other two directions. The bond-valence requirements of the two anions just bonded to C are satisfied by hydrogen bonding involving donor atoms both in the same structural unit and in different structural units. Thus in artinite, all linkage between structural units is through hydrogen bonding via (OH) and (H_2O) groups of the structural units; in addition, the (OH) groups allow polymerization in two directions within the structural unit, whereas the two types of (H_2O) groups allow polymerization in one and no directions, respectively, within the structural unit.

The (OH) and (H_2O) groups play a crucial role in controlling the polymerization of the structural unit in oxysalt minerals. Because of its very asymmetric distribution of bond-valences, the hydrogen atom can link to any strongly bonded unit, essentially preventing any further polymerization in that direction. Thus the *dimensionality* of the structural unit in a mineral is primarily controlled by the amount and role of hydrogen in the structure.

2.7.2 *(H_2O) groups bonded to interstitial cations*

Interstitial cations are usually large and of low charge. Generally, they are alkali or alkaline earth cations with Lewis acidities significantly less than those of the cations belonging to the structural unit. Consequently, (H_2O) can function as a ligand for these cations whereas (OH) cannot, as the cation to which it must bond cannot contribute enough bond-valence (i.e. about 1.0 v.u.)

for its bond-valence requirements to be satisfied. There are (at least) three possible reasons for (H_2O) groups to act as ligands for interstitial *cations*:

1. to satisfy the bond-valence requirements around the interstitial cation in cases where there are insufficient anions available from adjacent structural units;
2. to carry the bond-valence from the interstitial cation to a distant unsatisfied anion of an adjacent structural unit;
3. to act as bond-valence transformers between the interstitial cation and the anions of the structural unit; this is a mechanism of particular importance, and will be discussed separately later on.

A good example of (H_2O) of this kind is found in the structure of stringhamite (Hawthorne, 1985b), $[CaCu(SiO_4)](H_2O)$, the structure of which is illustrated in Figure 2.21. The structural unit is a sheet of corner-sharing (SiO_4) tetrahedra and square-planar (CuO_4) polyhedra, arranged parallel to (010). These sheets are linked together by interstitial Ca atoms; each Ca links to four anions from one sheet and one anion from the adjacent sheet. Presumably the Ca coordination number of [5], a value that is rare for Ca, is not adequate with regard to the satisfaction of local bond-valence requirements, and two (H_2O) groups complete the Ca coordination polyhedron. As shown in Figure 2.21, each

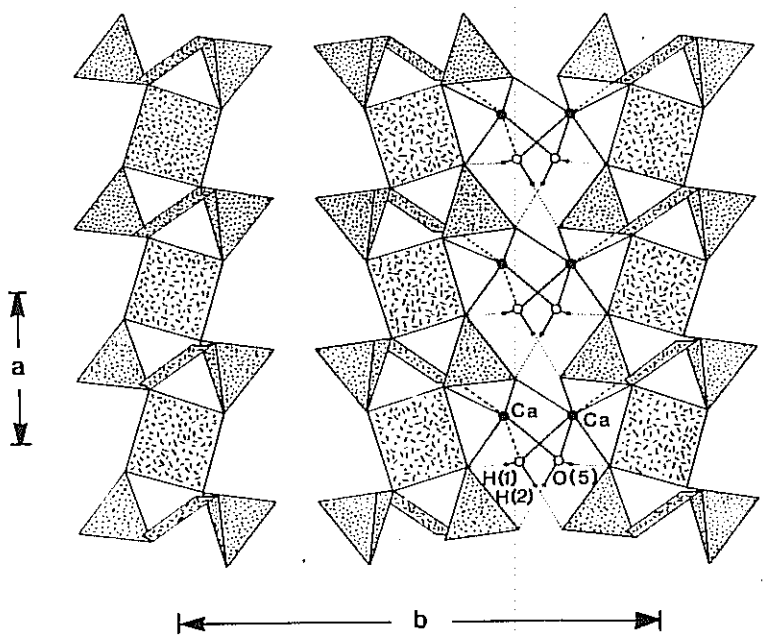

Figure 2.21 The crystal structure of stringhamite projected on to (001); interstitial species are omitted to the left of the diagram to emphasize the sheet-like nature of the structural unit.

(H_2O) group bonds to two Ca atoms, and also hydrogen bonds to anions in adjacent sheets, carrying the Ca bond-valence to anions which otherwise it could not reach. Thus the (H_2O) groups of this type, that is bonded only to interstitial cations, play a very different role from those (H_2O) groups that form part of the structural unit.

2.7.3 *Hydrogen-bonded interstitial (H_2O) groups*

In some structures, there are interstitial (H_2O) groups that are not bonded to any interstitial cations and yet participate in a well-defined hydrogen-bonding network. The (H_2O) groups of this sort act as both hydrogen-bond donors *and* hydrogen-bond acceptors. Any hydrogen-containing group (both (OH) and (H_2O) of the structural unit, interstitial (H_2O) bonded to interstitial cations, and interstitial (H_2O) groups not bonded to the structural unit or interstitial cations) can act as a hydrogen-bond donor to (H_2O) groups of this sort, and any anion or (H_2O) group can act as hydrogen-bond acceptor for such (H_2O) groups. Minerals with such hydrogen-bonding networks can be thought of as intermediate between anhydrous structures and clathrate structures.

A good example of such a structure is the mineral mandarinoite (Hawthorne, 1984b), $[Fe_2^{3+}(SeO_3)_3(H_2O)_3](H_2O)_3$, the structure of which is illustrated in Figure 2.22. The structural unit is a heteropolyhedral framework of corner-linking (SeO_3) triangular pyramids and (FeO_6) octahedra, with large cavities that are occupied by hydrogen-bonded (H_2O) groups in well-defined positions. Thus of the six (H_2O) groups in the formula unit, three are bonded to Fe^{3+} and are part of the structural unit; the three remaining (H_2O) groups are interstitial and not bonded to any cation at all, but held in place solely by a network of hydrogen bonds.

2.7.4 *Occluded (H_2O) groups*

Some structures contain (H_2O) groups that are not bonded to any cation and are not associated with any hydrogen-bonding scheme; normally such (H_2O) groups are located in holes within or between structural units. Such groups can occupy well-defined crystallographic positions, but their interaction with the rest of the structure is solely through a Van der Waals interaction.

A good example of such (H_2O) groups occurs in the structure of beryl. Alkali-free beryl can have non-bonded (H_2O) groups occurring in the channels of the framework structure. Most natural beryls contain alkali cations partly occupying sites within these channels, and these cations are bonded to channel (H_2O) groups. However, Hawthorne and Cerny (1977) have shown that most natural beryls contain (H_2O) groups in excess of that required to coordinate the channel cations, and hence some of the (H_2O) groups must be occluded rather than occurring as bonded components of the structure. Although such (H_2O) does not play a significant structural role, it can have important effects

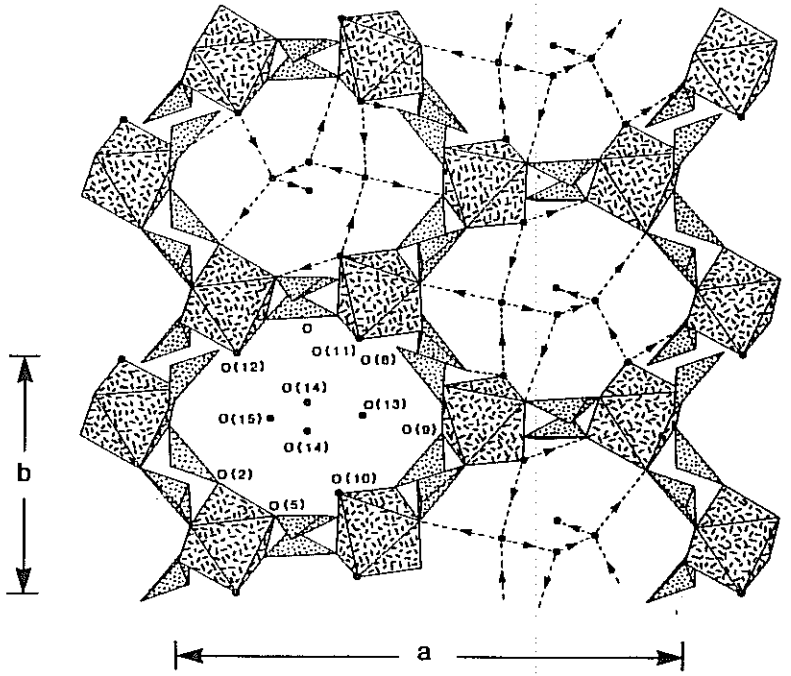

Figure 2.22 The crystal structure of mandarinoite projected on to (001); note the two different types of (H_2O) groups, one bonded to cations of the structural unit, and the other held in the structure by hydrogen-bonding only.

on such physical properties as specific gravity, optical properties (Cerny and Hawthorne, 1976) and dielectric behaviour.

2.8 (H_2O) as a bond-valence transformer

Consider a cation, M, that bonds to an anion X (Fig. 2.23(a)); the anion X receives a bond-valence of v valence units from the cation M. Consider a cation, M, that bonds to an (H_2O) group which in turn bonds to an anion X (Fig. 2.23(b)). In the second case, the oxygen receives a bond-valence of v valence units from the cation M, and its bond-valence requirements are satisfied by two short O–H bonds of valence (1 – v/2) valence units. To satisfy the bond-valence requirements around each hydrogen atom, each hydrogen forms at least one hydrogen bond with its neighbouring anions. In Figure 2.23(b), one of these hydrogen bonds is to the X anion which thus receives a bond-valence of one half what it received when it was bonded directly to the M cation. Thus the (H_2O) group has acted as a *bond-valence transformer*, causing one bond (bond-valence = v v.u.) to be split into two weaker bonds

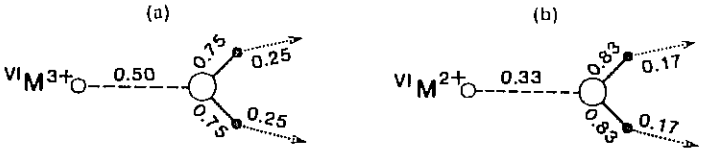

Figure 2.23 The transformer effect of (H_2O) groups: a cation bonds to an oxygen of an (H_2O) group, and the strong bond is split into two weaker bonds (hydrogen bonds) via the bond-valence requirements of the constituent H^+ and O^{2-} ions; this is shown for both M^{2+} and M^{3+} cations.

(bond-valence = v/2 v.u.). It is this *transformer effect* that is the key to understanding the role of interstitial (H_2O) in minerals.

2.9 Binary structural representation

It has been proposed (Hawthorne, 1985a; 1986) that the structural unit be treated as a (very) complex oxyanion. Within the framework of bond-valence theory, we can thus define a Lewis basicity for the structural unit in exactly the same way as we do for a more conventional oxyanion. We may then use the valence-matching principle to examine the interaction of the structural unit with the interstitial cations. In this way, we can get some quantitative insight into the weak bonding in minerals. It is worth emphasizing here that we have developed a *binary representation* that gives us a simple quantitative model of even the most complicated structure. We consider structures in this way not to convey the most complete picture of the bond topology, but to *express structure* in such a way that we may apply bond-valence arguments in an *a priori* fashion to problems of structural chemistry.

Let us look at goedkenite, $Sr_2[Al(PO_4)_2(OH)]$, the structural unit of which is shown in Figure 2.13(i). The bond network in the structural unit is shown in Figure 2.24 as a sketch of the smallest repeat fragment in the structural unit. There are 9 oxygens in this fragment (as indicated by the general $[M(T\phi_4)_2\phi]$ form of the structural unit), and the residual anionic charge is 4^-. In order to calculate the basicity of this structural unit, we must assign simple anion coordination numbers to the unit. Obviously, we must have an objective process for doing this, as the calculation of structural unit basicity hinges on this assignment. Fortunately, this assignment is fairly well-constrained by the general observation that most minerals have oxygen in [3]- or [4]-coordination; of course, it is easy to think of exceptions, quartz for example, but the fact that these exceptions are few 'proves the rule'. Normally it is adequate to use the coordination number [4]; however, there are the following exceptions:

1. Minerals with $M = 3^+$ and $T = 6^+$, for which the coordination number [3] is more appropriate.
2. A coordination number of [3] (including H atoms) is more appropriate for (H_2O), and is also used for (OH) when it is bonded to M^{3+} cations.

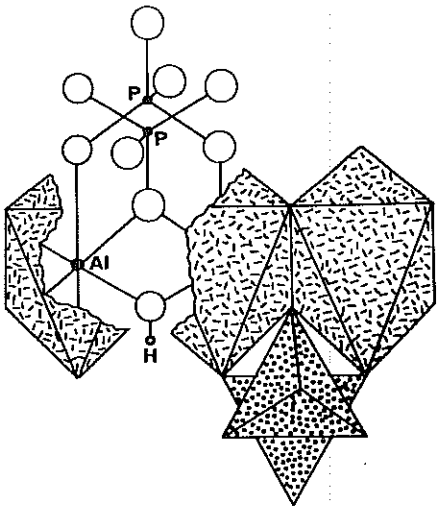

Figure 2.24 The bond network in the structural unit of goedkenite.

To attain an oxygen coordination number of [4], the cluster shown in Figure 2.24 needs an additional number of bonds from the interstitial cations. From the connectivity of the structural unit, the cluster of Figure 2.24 needs an additional 20 bonds; however, it will receive one (hydrogen) bond from an adjacent chain, which leaves 19 bonds to be received from the interstitial cations. These 19 bonds must come from 4^+ charges, and thus the average bond-valence required by the cluster is $4/19 = 0.22$ v.u.; this is the basicity of the structural unit in goedkenite. Examination of the table of Lewis acid strengths (Table 2.5) shows that the cations of appropriate Lewis acidity are Pb(0.20 v.u.), Sr(0.24 v.u.), and Ba(0.20 v.u.); in agreement with this, Sr is the interstitial cation in goedkenite. Note that Ca, with a Lewis basicity of 0.29 v.u., does not match with the Lewis basicity of the structural unit, and thus the valence-matching principle accounts for the fact that goedkenite has Sr rather than (the more common) Ca as the interstitial cation.

In this way of treating minerals, we have a simple binary interaction: the structural unit bonds with the interstitial cation(s). We may evaluate the stability of this interaction via the valence-matching principle, using the Lewis basicity of the structural unit and the Lewis acidity of the interstitial cation(s) as measures of their interaction. This reduces the most complex structure to a fairly simple representation, and looks at the interaction of its component features in a very simple but quantitative fashion.

2.10 Interstitial (H_2O) in minerals

So far, we have seen that (H_2O) plays a major role in controlling the character (dimensionality) of the structural unit; such (H_2O) is part of the structural unit and is stoichiometrically fixed by the topology of the unit connectivity. Interstitial (H_2O) is obviously very different in character. As we discussed previously, it may coordinate interstitial cations or it may occur solely as a component of a hydrogen-bonded network. Whichever is the case, the (H_2O) occupies fixed atomic positions and must play a role in the stability of the structure. The key to understanding this role is found in two distinct ideas of bond-valence theory:

1. the role of (H_2O) as a bond-valence transformer;
2. application of the valence-matching principle to the interaction between the structural unit and the interstitial cations.

Ideally, the valence of the bonds from the interstitial cations to the structural unit must match the Lewis basicity of that structural unit; if they do not match, then there cannot be a stable interaction and that particular structural arrangement will not occur. However, if the Lewis acidity of the interstitial cation is too large, the cation may bond to an interstitial (H_2O) group which acts as a bond-valence transformer (see Section 2.9), taking the strong bond and transforming it into two weaker bonds (Fig. 2.23). In this way, incorporation of interstitial (H_2O) into the structure can moderate the Lewis acidity of the interstitial cations such that the valence-matching principle is satisfied.

A good example of this is the ferric iron sulphate mineral botryogen, $Mg_2[Fe^{3+}_2(SO_4)_4(OH)_2(H_2O)_2](H_2O)_{10}$; why does this mineral have 10 interstitial (H_2O) groups per structural formula? The structural unit of botryogen is illustrated in Figure 2.13(k), and the coordinations of the various anions in the structural unit are shown in Table 2.9. Using the ideal coordination numbers discussed earlier (=[3] for all the simple anions in botryogen), the structural unit of botryogen needs an additional 26 bonds to achieve ideal coordination of all its simple anions. Six of these bonds will be hydrogen bonds from (OH) and (H_2O) groups within or in adjacent structural units, leaving 20 bonds needed from interstitial cations. Thus the Lewis basicity of the structural unit in botryogen is the charge divided by the number of required bonds: $4/20 = 0.20$ v.u. The interstitial cations in botryogen are Mg, with a Lewis acidity of 0.36 v.u. The valence-matching principle is violated, and a stable structure should not form. However, the interstitial Mg atoms are coordinated by $\{5(H_2O)+O\}$, and this will moderate the effective Lewis acidity of the cation via the transformer effect of (H_2O). Thus, the effective Lewis acidity of the 'complex cation' $\{Mg(H_2O)_5O\}$ is the charge divided by the number of bonds: $2/(5\times2+1) = 0.19$ v.u. The moderated Lewis acidity of the complex interstitial cation thus matches the Lewis basicity of the structural unit, and a stable mineral is formed.

Table 2.9 Details of H_2O 'of hydration' in botryogen

Botryogen: $Mg_2[Fe_2^{3+}(SO_4)_4(OH)_2(H_2O)_2](H_2O)_{10}$

Bonded atoms	Number of anions	Ideal coord. no.	Bonds needed for ideal coord.
S	10	3	2×10
$S + Fe^{3+}$	6	3	1×6
$2Fe^{3+} + H$	2	3	0
$Fe^{3+} + 2H$	2	3	0

Bonds needed to structural unit $= 2 \times 10 + 1 \times 6 = 26$
No. of H bonds to structural unit $= 2 \times 2 + 2 \times 1 = 6$
No. of additional bonds needed $= 26 - 6 = 20$
Charge on structural unit $= 4^-$
Lewis basicity of structural unit $= 4/20 = 0.20$ v.u.

Interstitial cation(s) is Mg
Mg coordination $= \{5(H_2O) + 0\}$
Bonds from Mg to structural unit $= 5 \times 2 + 1 = 11$
Effective Lewis acidity of Mg $= 2/\{5 \times 2 + 1\} = 0.19$ v.u.
The interstitial (H_2O) has moderated the Lewis acidity of the interstitial cation such that the valence-matching principle is satisfied

2.11 Bond-valence controls on interstitial cations

The structural unit is (usually) of anionic character, and thus has negative charge; this is neutralized by the presence of interstitial cations. Apart from the requirement of electroneutrality, the factors that govern the identity of the interstitial cations have been obscure. However, inspection of Tables 2.A2, 2.A3, and 2.A4 indicates that there must be controls on the identity of the interstitial cation. It is immediately apparent that different structural units are associated with different interstitial cations; thus $[M^{2+}(T^{5+}O_4)_2(H_2O)_2]$ chains (Fig. 2.13(a), Table 2.A3) always have Ca as the interstitial cation, whereas $[M^{2+}(T^{5+}O_4)_2(H_2O)]$ chains (Fig. 2.13(b), Table 2.A3) always have Pb^{2+} as the interstitial cation. Why is this so? If we were dealing with one or two very rare minerals, we might suspect that the difference is geochemically controlled; however, these are reasonably common minerals with significantly variable chemistry and paragenesis. We are forced to conclude that the control on interstitial cation type is crystal chemical rather than geochemical.

We find the answer to this problem in the application of the valence-matching principle to our binary representation of structure. The Lewis acidity of the interstitial cation must match up with the basicity of the structural unit. Thus it is not enough that the interstitial cation has the right valence; it must also have the right Lewis acidity. Let us examine the example outlined in the previous paragraph, that is the identity of the interstitial cations in the

$[M^{2+}(T^{5+}O_4)_2(H_2O)_2]$ and $[M^{2+}(T^{5+}O_4)_2(H_2O)]$ structures, using brandtite and brackebuschite as examples.

The situation for brandtite is shown in Table 2.10; counting the bonds within the structural unit indicates that an additional 20 bonds to the structural unit are needed to attain the requisite simple anion coordination numbers. Four of these bonds are hydrogen bonds from other structural units, leaving 16 bonds to be contributed by the interstitial cations. The residual charge on the structural unit is 4^- (per $[Mn^{2+}(AsO_4)_2(H_2O)_2]$ unit), and hence the basicity of the structural unit is $4/16 = 0.25$ v.u. Inspection of the Lewis acidity table (Table 2.5) shows that Ca has a Lewis acidity of 0.29 v.u., matching up with the Lewis basicity of the structural unit. Hence the valence-matching principle is satisfied, and $Ca_2[Mn^{2+}(AsO_4)_2(H_2O)_2]$ is a stable structure.

The situation for brackebuschite is also shown in Table 2.10; an additional 20 bonds are needed to satisfy the requisite simple anion coordination requirements. Two of these bonds are hydrogen bonds from adjacent structural units, leaving 18 bonds to be satisfied by the interstitial cations. The residual charge on the structural unit is 4^-, and hence the basicity of the structural unit is $4/18 = 0.22$ v.u. This value matches up quite well with the Lewis basicity of Pb^{2+} (0.20 v.u., see Table 2.5), the valence-matching principle is satisfied, and $Pb^{2+}[Mn^{2+}(V^{5+}O_4)_2(H_2O)]$ is a stable structure.

Table 2.10 Calculation of structural unit basicity for brandtite

Brandtite $= Ca_2[Mn^{2+}(AsO_4)_2(H_2O)_2]$ Structural unit $= [Mn^{[6]}(As^{[4]}O_4)_2(H^{[2]}_2O)_2]$
Number of bonds in structural unit $= 1 \times [6] + 2 \times [4] + 2 \times [2] = 18$
Number of bonds needed for [4]-coordination of all simple anions (except (H_2O) for which [3]-coordination is assigned) $= 8 \times [4] + 2 \times [3] = 38$
Number of additional bonds to structural unit to achieve this coordination $= 20$
Number of hydrogen bonds to structural unit $= 2 \times 2 = 4$
Therefore the number of bonds required from interstitial cations $= 20 - 4 = 16$
Charge on the structural unit $[Mn^{2+}(AsO_4)_2(H_2O)_2]$ in brandtite $= 4^-$
Lewis basicity of structural unit $=$ charge/bonds $= 4/16 = 0.25$ v.u.
This basicity matches most closely with the Lewis acidity of Ca at 0.27 v.u.
Thus the formula of brandtite is $Ca_2[Mn(AsO_4)_2(H_2O)_2]$

Brackebuschite $= Pb_2[Mn^{2+}(VO_4)_2(H_2O)]$ Structural unit $= [Mn^{[6]}(V^{[4]}O_4)_2(H^{[2]}_2O)]$
Number of bonds in structural unit $= 1 \times [6] + 2 \times [4] + 2 \times [1] = 16$
Number of bonds needed for [4]-coordination of all simple anions (including (H_2O) which is [4]-coordinated in this structural unit) $= 9 \times [4] = 36$
Number of additional bonds to structural unit to achieve this coordination $= 20$
Number of hydrogen bonds to structural unit $= 2$
Number of bonds required from interstitial cations $= 18$
Charge on the structural unit $[Mn^{2+}(VO_4)_2(H_2O)]$ in brackebuschite $= 4^-$
Lewis basicity of structural unit $=$ charge/bonds $= 4/18 = 0.22$ v.u.
This basicity matches most closely with the Lewis acidity of Pb at 0.20 v.u.
Thus the formula of brackebuschite is $Pb_2[Mn(VO_4)_2(H_2O)]$

Now that we understand the basis of this selectivity of interstitial cations, some very interesting geological questions become apparent. Does the form of the structural unit dictate the identity of the interstitial cations, or does the availability of a particular interstitial cation dictate the form of the structural unit? Does the pH of the environment affect the form of the structural unit or the amount of interstitial (H_2O) incorporated into the structure? Are there synergetic interactions between these factors? Using bond-valence theory in conjunction with the topological characteristics of the structural unit, we can begin to investigate some of these questions that previously we have had no conceptual basis to think about.

2.12 Structural controls on mineral paragenesis

2.12.1 Magnesium sulphate minerals

The magnesium sulphate minerals are important phases in many marine salt deposits, and these parageneses can be very complicated. Common minerals in these deposits are given in Table 2.11, together with an indication of the character of the structural unit and its Lewis basicity. The paragenetic scheme shown in Figure 2.25 was constructed from an examination of natural occurrences, together with consideration of their phase relations in aqueous solutions. The arrows in Figure 2.25 indicate a change in the crystallizing phase from an aqueous solution of the bulk composition of the previously crystallizing phase, and/or an alteration sequence. Obviously, these equilibria will be specifically dependent on temperature, bulk composition and pH, but the natural assemblages suggest that the scheme of Figure 2.25 corresponds reasonably well to the general case.

Table 2.11 Common magnesium sulphate minerals

Mineral	Formula	Structural unit	Unit basicity (v.u.)
Langbeinite	$K_2Mg_2(SO_4)_3$	Infinite framework	0.11
Loeweite	$Na_{12}Mg_7(SO_4)_{13} \cdot 15H_2O$	Infinite framework	0.14
Vanthoffite	$Na_6Mg(SO_4)_4$	Infinite sheet	0.14
Polyhalite	$K_2Ca_2Mg(SO_4)_4 \cdot 2H_2O$	Finite cluster	0.21
Kieserite	$Mg(SO_4) \cdot H_2O$	Infinite framework	0.00
Leonite	$K_2Mg(SO_4)_2 \cdot 4H_2O$	Finite cluster	0.14
Bloedite	$Na_2Mg(SO_4)_2 \cdot 4H_2O$	Finite cluster	0.14
Pentahydrite	$Mg(SO_4) \cdot 5H_2O$	Infinite chain	0.00
Hexahydrite	$Mg(SO_4) \cdot 6H_2O$	Isolated polyhedra	0.00
Picromerite	$K_2Mg(SO_4)_2 \cdot 6H_2O$	Isolated polyhedra	0.13
Epsomite	$Mg(SO_4) \cdot 7H_2O$	Isolated polyhedra	0.00

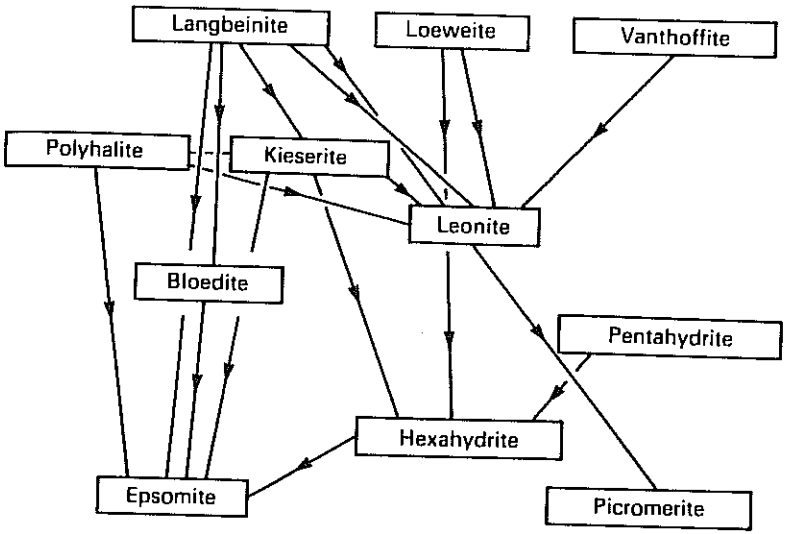

Figure 2.25 Approximate paragenetic scheme for $A_x[Mg_x(SO_4)_y\phi_z]$ salt minerals. The arrows denote progressive crystallization and/or alteration.

It is apparent from inspection of Table 2.11 that there is a gradual depolymerization of the structural unit down through the paragenetic sequence of Figure 2.25. This change is effected by the incorporation of increasing amounts of (H_2O) into the structural units, the (H_2O) groups essentially blocking further polymerization where they attach to the structural unit. This decrease in the polymerization of the structural unit is also accompanied by a decrease in the basicity of the structural unit (Table 2.11, Fig. 2.26). This has the effect of changing the character of the interstitial cations, which are gradually decreasing in Lewis acidity, until at the last stages of the crystalliz-

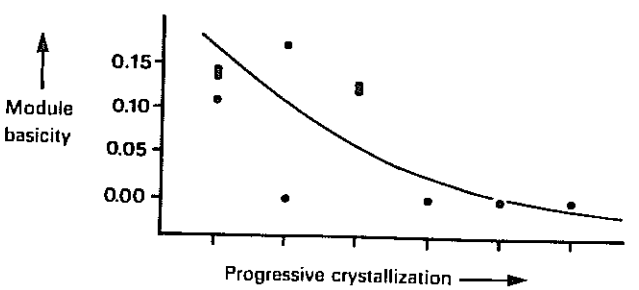

Figure 2.26 Change in character of structural unit with progressive crystallization for the minerals of Figure 2.25.

ation sequence, there are no interstitial cations left, and the structural units are neutral.

Figure 2.27 shows the evolution of the character of the structural units. For a specific Lewis basicity, there is a gradual de-polymerization of the structural unit with progressive crystallization. The pattern exhibited by Figure 2.27 suggests a specific control on the character of the crystallizing mineral(s). Crystallization begins with the formation of a structural unit of maximum connectivity and the highest possible Lewis basicity consonant with the Lewis acidity of the most acid cation available. With continued crystallization, the dimension of polymerization of the structural unit gradually decreases while the Lewis basicity of the structural units is maintained. As the most acid cation

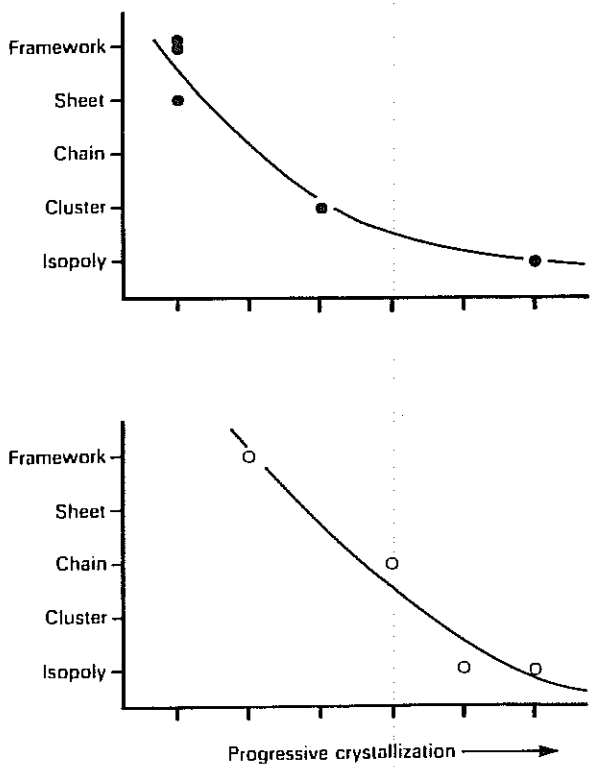

Figure 2.27 Change in character of structural unit with progressive crystallization for the minerals of Figure 2.25; the upper figure is for minerals with a Lewis basicity of ~0.15 v.u. for their structural units, the lower figure is for minerals with a Lewis basicity of zero for their structural units.

becomes depleted, there is the beginning of crystallization of structural units of lower basicity and the incorporation of less acid cations into the structure. Again the degree of polymerization of the structural units decreases with progressive crystallization, but the basicity of the structural units is maintained until the cations of corresponding acidity are gone. This process repeats itself with structural units and interstitial cations of progressively decreasing basicity and acidity respectively, until we reach the final stage when the structural units have zero basicity and there are no interstitial cations in the resulting minerals. Note that at any stage in the crystallization process structural units of differing basicities may be crystallizing simultaneously, the resulting minerals incorporating very different interstitial cations; however, the connectivities (dimensions of polymerization) of the structural units are very different. This scheme seems to work quite well for these minerals, and one can make all sorts of inferences about possible complexing in solution and crystallization mechanisms. It will be interesting to see how well this scheme works in more complicated systems.

2.13 Summary

Here I have tried to develop a global approach to questions of stability and paragenesis of oxide and oxysalt minerals. The fundamental basis of the approach relates to the energetic content of the bond topology of a structure. Bond topology has a major effect on the energetics of a structure, suggesting that major trends in structure stability, properties, and behaviour should be systematically related to the coordination geometry and polyhedral linkage of a structure. Combination of these ideas with bond-valence theory (a very simple form of molecular orbital theory) allows a simple binary representation of even the most complex structure: a (usually anionic) structural unit that interacts with (usually cationic or neutral) interstitial species to form the complete structure. This interaction can be quantitatively examined in terms of the Lewis basicities and acidities of the binary components, and such chemical variables as interstitial cation chemistry and 'water' of hydration can be quantitatively explained. Examination of a few complex mineral parageneses, together with the topological character of the structural unit, indicates that the latter has a major control on the sequence of crystallization of the constituent minerals. In addition, the persistence of particular fundamental building blocks in series of associated minerals suggests that such clusters may occur as complex species in associated hydrothermal and saline fluids.

The principal idea behind this work is to develop an approach that is reasonably transparent to chemical and physical intuition, and that can be applied to large numbers of very complex structures in geological environments. Mineralogy is currently absorbing a large number of 'theoretical' techniques from physics and chemistry, examining aspects of (fairly simple) minerals. One of the dangers with this is that it is easy to become lost in the

technical complexities of the computational approach, and the basic physics and chemistry of what is going on can become lost; one is merely doing a numerical experiment. By and large, mineralogists have not fallen into this trap; in particular, the work of G. V. Gibbs and colleagues has continually pursued the important energetic mechanisms operative in minerals. However, I feel that there is also room for a much simpler approach that addresses more global aspects of complex minerals, working well below the 'Pauling point' rather than above it. These ideas tend to be more intuitive and only semi-quantitative, but seem to be capable of organizing a large amount of factual information into a coherent framework, and also provide a basis for thinking about many questions that were intractable to previous approaches.

Acknowledgements

I have been strongly influenced by the ideas of I. David Brown, Jeremy K. Burdett, and Paul B. Moore; as a result, they can take the blame for any shortcomings of the present work. This work was supported by the Natural Sciences and Engineering Council of Canada in the form of an Operating Grant to the author.

Appendix

Table 2.A1 $M(T\phi_4)\phi_n$ and $M(T\phi_4)_2\phi_n$ minerals based on isolated $M\phi_6$ octahedra and $T\phi_4$ tetrahedra

$M(T\phi_4)\phi_n$ mineral	Formula	$M(T\phi_4)_2\phi_n$ mineral	Formula
Bianchite	$[Zn(H_2O)_6][SO_4]$	Amarillite	$Na[Fe^{3+}(SO_4)_2(H_2O)_6]$
Ferrohexahydrite	$[Fe^{2+}(H_2O)_6][SO_4]$	Tamarugite	$Na[Al(SO_4)_2(H_2O)_6]$
Hexahydrite	$[Mg(H_2O)_6][SO_4]$		
Moorhouseite	$[Co(H_2O)_6][SO_4]$	Mendozite	$Na_2[Al(SO_4)_2(H_2O)_6](H_2O)_5$
Nickel-hexahydrite	$[Ni(H_2O)_6][SO_4]$	Kalinite	$K[Al(SO_4)_2(H_2O)_6](H_2O)_5$
Reigersite	$[Ni(H_2O)_6][SO_4]$	Sodium alum	$Na[Al(SO_4)_2(H_2O)_6](H_2O)_6$
Khademite	$[Al(H_2O)_5F][SO_4]$	Potassium alum	$K[Al(SO_4)_2(H_2O)_6](H_2O)_6$
Epsomite	$[Mg(H_2O)_6][SO_4](H_2O)$	Tschermigite	$NH_4[Al(SO_4)_2(H_2O)_6](H_2O)_6$
Goslarite	$[Zn(H_2O)_6][SO_4](H_2O)$	Apjohnite	$Mn[Al(SO_4)_2(H_2O)_6](H_2O)_{10}$
Morenosite	$[Ni(H_2O)_6][SO_4](H_2O)$	Bilinite	$Fe^{2+}[Fe^{3+}(SO_4)_2(H_2O)_6](H_2O)_{10}$
		Dietrichite	$Zn[Al(SO_4)_2(H_2O)_6](H_2O)_{10}$
Bieberite	$[Co(H_2O)_6][SO_4](H_2O)$	Halotrichite	$Fe^{2+}[Al(SO_4)_2(H_2O)_6](H_2O)_{10}$
Boothite	$[Cu(H_2O)_6][SO_4](H_2O)$	Pickeringite	$Mg[Al(SO_4)_2(H_2O)_6](H_2O)_{10}$
Mallardite	$[Mn(H_2O)_6][SO_4](H_2O)$	Redingtonite	$Fe^{2+}[Cr(SO_4)_2(H_2O)_6](H_2O)_{10}$
Melanterite	$[Fe^{2+}(H_2O)_6][SO_4](H_2O)$	Auberiite	$Cu^{2+}[Al(SO_4)_2(H_2O)_6]Cl(H_2O)_8$
Zinc-melanterite	$[Zn(H_2O)_6][SO_4](H_2O)$	Boussingaultite	$(NH_4)_2[Mg(SO_4)_2(H_2O)_6]$
		Cyanochroite	$K_2[Cu^{2+}(SO_4)_2(H_2O)_6]$
Phosphorroesslerite	$[Mg(H_2O)_6][PO_3(OH)](H_2O)$		
		Mohrite	$(NH_4)_2[Fe^{2+}(SO_4)_2(H_2O)_6]$
Roesslerite	$[Mg(H_2O)_6][AsO_3(OH)](H_2O)$		
		Picromerite	$K_2[Mg(SO_4)_2(H_2O)_6]$
Struvite	$NH_4[Mg(H_2O)_6][PO_4]$		
		Despujolsite	$Ca_3[Mn^{4+}(SO_4)_2(OH)_6][H_2O)_3$
		Fleischerite	$Pb_3[Ge(SO_4)_2(OH)_6][H_2O)_3$
		Schuenerite	$Ca_3[Ge(SO_4)_2(OH)_6][H_2O)_3$

Table 2.A2 $M(T\phi_4)\phi_n$ and $M(T\phi_4)_2\phi_n$ minerals based on finite clusters of $M\phi_6$ octahedra and $T\phi_4$ tetrahedra

$M(T\phi_4)\phi_n$ mineral	Formula	$M(T\phi_4)_2\phi_n$ mineral	Formula
Aplowite	$[Co(SO_4)(H_2O)_4]$	Anapaite	$Ca_2[Fe^{2+}(PO_4)_2(H_2O)_4]$
Boyleite	$[Zn(SO_4)(H_2O)_4]$	Bloedite	$Na_2[Mg(SO_4)_2(H_2O)_4]$
Ilesite	$[Mn(SO_4)(H_2O)_4]$	Leonite	$K_2[Mg(SO_4)_2(H_2O)_4]$
Rozenite	$[Fe^{2+}(SO_4)(H_2O)_4]$	Schertelite	$(NH_4)_2[Mg(PO_3OH)_2(H_2O)_4]$
Starkeyite	$[Mg(SO_4)(H_2O)_4]$	Roemerite	$Fe^{2+}[Fe^{3+}(SO_4)_2(H_2O)_4]_2(H_2O)_6$
Morinite	$Ca_2Na[Al_2(PO_4)_2F_4(OH)(H_2O)_2]$	Metavoltine	$K_2Na_6Fe^{2+}[Fe_3^{3+}(SO_4)_6O(H_2O)_3]_2(H_2O)_{12}$

Table 2.A3 $M(T\phi_4)\phi_n$ and $M(T\phi_4)_2\phi_n$ minerals based on infinite chains of $M\phi_6$ octahedra and $T\phi_4$ tetrahedra

$M(T\phi_4)\phi_n$ mineral	Formula	$M(T\phi_4)_2\phi_n$ mineral	Formula
Chalcanthite	$[Cu(SO_4)(H_2O)_4](H_2O)$	Brandtite	$Ca_2[Mn(AsO_4)_2(H_2O)_2]$
Jokokuite	$[Mn(SO_4)(H_2O)_4](H_2O)$	Krohnkite	$Na_2[Cu(SO_4)_2(H_2O)_2]$
Pentahydrite	$[Mg(SO_4)(H_2O)_4](H_2O)$	Roselite	$Ca_2[Co(AsO_4)_2(H_2O)_2]$
Siderotil	$[Fe^{2+}(SO_4)(H_2O)_4](H_2O)$	Cassidyite	$Ca_2[Ni(PO_4)_2(H_2O)_2]$
Liroconite	$Cu_2[Al](AsO_4)(OH)_4](H_2O)_4$	Collinsite	$Ca_2[Mg(PO_4)_2(H_2O)_2]$
Brassite	$[Mg(AsO_3(OH))(H_2O)_4]$	Gaitite	$Ca_2[Zn(AsO_4)_2(H_2O)_2]$
		Talmessite	$Ca_2[Mg(AsO_4)_2(H_2O)_2]$

Butlerite	$[Fe^{3+}(SO_4)(OH)(H_2O)_2]$	Fairfieldite	$Ca_2[Mn(PO_4)_2(H_2O)_2]$
Parabutlerite	$[Fe^{3+}(SO_4)(OH)(H_2O)_2]$	Messelite	$Ca_2[Fe^{2+}(PO_4)_2(H_2O)_2]$
Childrenite	$Mn^{2+}[Al(PO_4)(OH)_2(H_2O)]$	Tancoite	$Na_2LiH[Al(PO_4)_2(OH)]$
Eosphorite	$Fe^{2+}[Al(PO_4)(OH)_2(H_2O)]$	Sideronatrite	$Na_2[Fe^{3+}(SO_4)_2(OH)](H_2O)_3$
Uklonskovite	$Na[Mg(SO_4)(OH)(H_2O)_2]$	Jahnsite	$CaMnMg_2[Fe^{3+}(PO_4)_2(OH)]_2(H_2O)_8$
Fibroferrite	$[Fe^{3+}(SO_4)(OH)(H_2O)_2](H_2O)_4$	Whiteite	$CaFe^{2+}Mg_2[Al(PO_4)_2(OH)]_2(H_2O)_8$
Chlorothionite	$K_2[Cu(SO_4)Cl_2]$	Lun'okite	$Mn_2Mg_2[Al(PO_4)_2(OH)]_2(H_2O)_8$
Linarite	$Pb[Cu(SO_4)(OH)_2]$	Overite	$Ca_2Mg_2[Al(PO_4)_2(OH)]_2(H_2O)_8$
Schmiederite	$Pb_2[Cu_2(SeO_3)(SeO_4)(OH)_4]$	Segelerite	$Ca_2Mg_2[Fe^{3+}(PO_4)_2(OH)]_2(H_2O)_8$
Amarantite	$[Fe_2^{3+}(SO_4)_2O(H_2O)_4](H_2O)_3$	Wilhelmvierlingite	$Ca_2Mn_2[Fe^{3+}(PO_4)_2(OH)]_2(H_2O)_8$
Hohmannite	$[Fe_2^{3+}(SO_4)_2O(H_2O)_4](H_2O)_4$	Guildite	$Cu^{2+}[Fe^{3+}(SO_4)_2(OH)](H_2O)_4$
Fornacite	$Pb_2[Cu(AsO_4)(CrO_4)(OH)]$	Yftisite	$Y_4[Ti(SiO_4)_2O](F,OH)_6$
Molybdofornacite	$Pb_2[Cu(AsO_4)(MoO_4)(OH)]$	Arsenbrackebuschite	$Pb_2[Fe^{2+}(AsO_4)_2(H_2O)]$
Tornebohmite	$(RE)_2[Al(SiO_4)_2(OH)]$	Arsentsumebite	$Pb_2[Cu(SO_4)(AsO_4)(OH)]$
Ransomite	$Cu[Fe^{3+}(SO_4)_2(H_2O)]_2(H_2O)_4$	Brackebuschite	$Pb_2[Mn(VO_4)_2(H_2O)]$
Krausite	$K[Fe^{3+}(SO_4)_2(H_2O)]$	Gamagarite	$Ba_2[(Fe^{3+}, Mn)(VO_4)_2(OH, H_2O)]$
Botryogen	$Mg_2[Fe_2^{3+}(SO_4)_4(OH)_2(H_2O)_2](H_2O)_{10}$	Goedkenite	$Sr_2[Al(PO_4)_2(OH)]$
Zincbotryogen	$Zn_2[Fe_2^{3+}(SO_4)_4(OH)_2(H_2O)_2](H_2O)_{10}$	Tsumebite	$Pb_2[Cu(PO_4)(SO_4)(OH)]$
		Vauquelinite	$Pb_2[Cu(PO_4)(CrO_4)(OH)]$

Table 2.A4 $M(T\phi_4)\phi_n$ and $M(T\phi_4)_2\phi_n$ minerals based on infinite sheets of $M\phi_6$ octahedra and $T\phi_4$ tetrahedra

$M(T\phi_4)\phi_n$ mineral	Formula	$M(T\phi_4)_2\phi_n$ mineral	Formula
Tsumcorite	$Pb[(Zn, Fe^{3+})(AsO_4)(H_2O, OH)]_2$	Rhomboclase	$(H_5O_2)[Fe^{3+}(SO_4)_2(H_2O)_2]$
Bermanite	$Mn^{2+}[Mn^{3+}(PO_4)(OH)]_2(H_2O)_4$	Olmsteadite	$KFe_2^{3+}[Nb(PO_4)_2O_2](H_2O)_2$
Foggite	$Ca[Al(PO_4)(OH)_2](H_2O)$	Brianite	$Na_2Ca[Mg(PO_4)_2]$
		Merwinite	$Ca_3[Mg(SiO_4)_2]$
Arthurite	$Cu[Fe^{3+}(AsO_4)(OH)]_2(H_2O)_4$		
Earlshannonite	$Mn^{2+}[Fe^{3+}(PO_4)(OH)]_2(H_2O)_4$	Yavapaite	$K[Fe^{3+}(SO_4)_2]$
Ojuelaite	$Zn[Fe^{3+}(AsO_4)(OH)]_2(H_2O)_4$		
		Bafertisite	$BaFe^{2+}[Ti(Si_2O_7)O_2]$
Whitmoreite	$Fe^{2+}[Fe^{3+}(PO_4)(OH)]_2(H_2O)_4$		
		Pyrophyllite	$[AlSi_2O_5(OH)]$
Krautite	$[Mn^{2+}(AsO_3OH)(H_2O)]$		
		Dioctahedral micas	(M^+, M^{2+}) $[(M^{3+}, M^{2+})(Si, Al)_2O_5(OH)]_2$
Fluckite	$[CaMn^{2+}(AsO_3OH)_2(H_2O)_2]$		
		Ephesite	$NaLi[Al(Si, Al)_2O_5(OH)]_2$
Co-Koritnigite	$[Co(AsO_3OH)(H_2O)]$		
		Taenolite	$KLi[MgSi_2O_5(OH)]_2$
Koritnigite	$[Zn(AsO_3OH)(H_2O)]$		
		Dioctahedral smectites	(M^+, H_2O) $[(M^{3+}, M^{2+})(Si, Al)_2O_5(OH)]_2$
Kaolinite	$[Al_2Si_2O_5(OH)_4]$		
Dickite	$[Al_2Si_2O_5(OH)_4]$	Bramallite	$(M^+, H_2O)_x$ $[(Al, Mg, Fe)(Si, Al)_2O_5(OH)]_2$
Nacrite	$[Al_2Si_2O_5(OH)_4]$	Hydromica	$(M^+, H_2O)_x[Al(Si, Al)_2O_5(OH)]_2$
Endellite	$[Al_2Si_2O_5(OH)_4] \cdot 2(H_2O)$	Illite	$(M^+, H_2O)_x$ $[(Al, Mg, Fe)(Si, Al)_2O_5(OH)]_2$
Halloysite	$[Al_2Si_2O_5(OH)_4]$		
		Goldichite	$K_2[Fe_2^{3+}(SO_4)_4(H_2O)_4](H_2O)_4$
Arseniosiderite	$Ca_2[Fe_3^{3+}(AsO_4)_3O_2](H_2O)_3$		
Kolfanite	$Ca_2[Fe_3^{3+}(AsO_4)_3O_2](H_2O)_2$		
Mitridatite	$Ca_2[Fe_3^{3+}(PO_4)_3O_2](H_2O)_3$		
Robertsite	$Ca_2[Mn_3^{3+}(PO_4)_3O_2](H_2O)_3$		
Newberyite	$[Mg(PO_3OH)(H_2O)_3]$		
Minyulite	$K[Al_2(PO_4)_2F(H_2O)_4]$		
Gordonite	$Mg[Al_2(PO_4)_2(OH)_2(H_2O)_2](H_2O)_4 \cdot 2(H_2O)$		
Laueite	$Mn^{2+}[Fe_2^{3+}(PO_4)_2(OH)_2(H_2O)_2](H_2O)_4 \cdot 2(H_2O)$		
Paravauxite	$Fe^{2+}[Al_2(PO_4)_2(OH)_2(H_2O)_2](H_2O)_4 \cdot 2(H_2O)$		
Sigloite	$(Fe^{3+}, Fe^{2+})[Al_2(PO_4)_2(OH)_2(H_2O)_2](H_2O, OH)_4 \cdot 2(H_2O)$		
Ushkovite	$Mg[Fe_2^{3+}(PO_4)_2(OH)_2(H_2O)_2](H_2O)_4 \cdot 2(H_2O)$		
Stewartite	$Mn^{2+}[Fe_2^{3+}(PO_4)_2(OH)_2(H_2O)_2](H_2O)_4 \cdot 2(H_2O)$		
Pseudolaueite	$Mn^{2+}[Fe^{3+}(PO_4)(OH)(H_2O)]_2(H_2O)_4 \cdot 2(H_2O)$		
Strunzite	$Mn^{2+}[Fe^{3+}(PO_4)(OH)(H_2O)]_2(H_2O)_4$		
Ferrostrunzite	$Fe^{2+}[Fe^{3+}(PO_4)(OH)(H_2O)]_2(H_2O)_4$		
Metavauxite	$Fe^{2+}[Al(PO_4)(OH)(H_2O)]_2(H_2O)_6$		

Table 2.A5 $M(T\phi_4)\phi_n$ and $M(T\phi_4)_2\phi_n$ minerals based on infinite frameworks of $M\phi_6$ octahedra and $T\phi_4$ tetrahedra

$M(T\phi_4)\phi_n$ mineral	Formula
Bonattite	$[Cu(SO_4)(H_2O)_3]$
Kolbeckite	$[Sc(PO_4)(H_2O)_2]$
Metavariscite	$[Al(PO_4)(H_2O)_2]$
Phosphosiderite	$[Fe^{3+}(PO_4)(H_2O)_2]$
Mansfieldite	$[Al(AsO_4)(H_2O)_2]$
Scorodite	$[Fe^{3+}(AsO_4)(H_2O)_2]$
Strengite	$[Fe^{3+}(PO_4)(H_2O)_2]$
Variscite	$[Al(PO_4)(H_2O)_2]$
Kainite	$K_4[Mg_4(SO_4)_4(H_2O)_{11}]Cl_4$
Amblygonite	$Li[Al(PO_4)F]]$
Montebrasite	$Li[Al(PO_4)OH]$
Tavorite	$Li[Fe^{3+}(PO_4)OH]$
Durangite	$Na[Al(AsO_4)F]$
Isokite	$Ca[Mg(PO_4)F]$
Lacroixite	$Na[Al(PO_4)F]$
Malayaite	$Ca[Sn^{4+}(SiO_4)O]$
Panasquereite	$Ca[Mg(PO_4)OH]$
Tilasite	$Ca[Mg(AsO_4)F]$

$M(T\phi_4)_2\phi_n$ mineral	Formula
Keldyshite	$(Na,H_3O)[Zr(Si_2O_7)]$
Parakeldyshite	$Na[Zr(Si_2O_7)]$
Nenadkevichite	$Na_2[Nb(Si_2O_6)OH](H_2O)_2$
Labuntsovite	$K_2[Ti(Si_2O_6)OH](H_2O)_2$
Batisite	$Na_2Ba[Ti(Si_2O_6)O]_2$
Shcherbakovite	$K_2Ba[(Ti, Nb)(Si_2O_6)O]_2$
Alkali pyroxenes	$M^+[M^{3+}(Si_2O_6)]$
Calic pyroxenes	$Ca[M^{2+}(Si_2O_6)]$
Lavenite	$(Na, Ca)_3[Zr(Si_2O_7)O]F$
Wohlerite	$Na_2Ca_4[ZrNb(Si_2O_7)_2O_2]F$
Rosenbuschite	$(Ca, Na)_2[Zr_2Ti_2(Si_2O_7)_4O_2F_2]F_4$

$M(T\phi_4)\phi_n$ Mineral	Formula
Barbosalite	$Fe^{2+}[Fe^{3+}(PO_4)OH]_2$
Lazulite	$Mg[Al(PO_4)OH]_2$
Scorzalite	$Fe^{2+}[Al(PO_4)OH]_2$
Lawsonite	$Ca[Al_2(Si_2O_7)(OH)_2](H_2O)$

Titanite-$P2_1/c$	$Ca[Ti(SiO_4)O]$
Titanite-C2/c	$Ca[(Ti, Al, Fe)(SiO_4)O]$
Dwornikite	$[Ni(SO_4)(H_2O)]$
Gunningite	$[Zn(SO_4)(H_2O)]$
Kieserite	$[Mg(SO_4)(H_2O)]$
Poitevinite	$[Cu(SO_4)(H_2O)]$
Szmikite	$[Mn^{2+}(SO_4)(H_2O)]$
Szomolnokite	$[Fe^{2+}(SO_4)H_2O)]$
Adelite	$Ca[Mg(AsO_4)OH]$
Austinite	$Ca[Zn(AsO_4)OH]$
Conichalcite	$Ca[Cu(AsO_4)OH]$
Duftite	$Pb[Cu(AsO_4)OH]$
Gabrielsonite	$Pb[Fe^{2+}(AsO_4)OH]$
Vuagnatite	$Ca[Al(SiO_4)OH]$
Arsendescloizite	$Pb[Zn(AsO_4)OH$
Calciovolborthite	$Ca[Cu(VO_4)OH]$
Cechite	$Pb[Fe^{2+}(VO_4)OH]$
Descloizite	$Pb[Zn(VO_4)OH]$
Mottramite	$Pb[Cu(VO_4)OH]$
Dioptase	$[Cu_6(Si_6O_{18})(H_2O)_6]$
Veszelyite	$[Cu_2(ZnPO_4OH)(OH)_2(H_2O)_2]$
Holdenite	$[Mn_6^{3+}(Zn_3As_2SiO_{12}(OH)_8)]$
Alluaudite	$(Na, Ca)[Fe^{2+}(Mn, Fe, Mg)_2(PO_4)_3]$
Hagendorfite	$(Na, Ca)[Mn^{2+}(Fe, Mg)_2(PO_4)_3]$
Maghagendorfite	$Na[Mn^{2+}(Mg, Fe)_2(PO_4)_3]$
Varulite	$(Na, Ca)[Mn^{2+}(Mn, Fe)_2(PO_4)_3]$
Plancheite	$[Cu_8(Si_8O_{22})(OH)_4(H_2O)]$
Tiragalloite	$[Mn_4(AsSi_3O_{12}(OH)]$
Medaite	$[Mn_6(VSi_5O_{18})(OH)]$
Zoisite	$Ca_2[Al_3(SiO_4)(Si_2O_7)O(OH)]$
Allanite	$(Ce, Ca)_2[Al_3(SiO_4)(Si_2O_7)O(OH)]$
Allanite-(Y)	$(Y, Ce, Ca)_2[Al_3(SiO_4)(Si_2O_7)O(OH)]$
Clinozoisite	$Ca_2[Al_3(SiO_4)(Si_2O_7)O(OH)]$
Epidote	$Ca_2[Fe^{3+}(SiO_4)(Si_2O_7)O(OH)]$
Hancockite	$(Pb, Ca)_2[Al_3(SiO_4)(Si_2O_7)O(OH)]$
Piemontite	$Ca_2[Mn_3^{3+}(SiO_4)(Si_2O_7)O(OH)]$

$M(T\phi_4)\phi_n$ mineral	Formula	$M(T\phi_4)_2\phi_n$ mineral	Formula
Pyrobelonite	$Pb[Mn(VO_4)OH]$		
		Orthoenstatite	$[Mg(SiO_3)]$
Jagowerite	$Ba[Al(PO_4)OH]_2$		
		Hypersthene	$[(Mg,Fe^{2+})(SiO_3)]$
Melonjosephite	$Ca[Fe^{2+}Fe^{3+}(PO_4)_2OH]$	Orthoferrosilite	$[Fe^{2+}(SiO_3)]$
Bertossaite	$CaLi_2[Al(PO_4)OH]_4$	Clinoenstatite	$[Mg(SiO_3)]$
Palermoite	$SrLi_2[Al(PO_4)OH]_4$	Clinohypersthene	$[(Mg,Fe^{2+})(SiO_3)]$
		Clinoferrosilite	$[Fe^{2+}(SiO_3)]$
Carminite	$Pb[Fe^{3+}(AsO_4)OH]_2$		
Leucophosphite	$K[Fe_2^{3+}(PO_4)_2(OH)(H_2O)](H_2O)_2$		
Ferropumpellyite	$Ca_2[Al_2(Al,Fe^{2+})(SiO_4)(Si_2O_7)(OH)_2(OH,H_2O)]$		
Jugoldite	$Ca_2[Fe_2^{3+}(Fe^{3+},Fe^{2+})(SiO_4)(Si_2O_7)(OH)_2(OH,H_2O)]$		
Pumpellyite	$Ca_2[Al_2(Al,Mg)(SiO_4)(Si_2O_7)(OH)_2(OH,H_2O)]$		
Shuiskite	$Ca_2[Cr_2(Al,Mg)(SiO_4)(Si_2O_7)(OH)_2(OH,H_2O)]$		
Ardennite	$(Mn,Ca)_4[Al_4(Mg,Al)_2(SiO_4)_2(Si_3O_{10})(AsO_4,VO_4)(OH)_6]$		

References

Akao, M. and Iwai S. (1977) The hydrogen bonding of artinite. *Acta Crystallographica* **B33**, 3951–3.

Alhright, T. A., Burdett, J. K., and Whangbo, M. H. (1985) *Orbital Interactions in Chemistry*, Wiley-Interscience, New York.

Allmann, R. (1975) Beziehungen zwischen Bindungslangen und Bindungsstarken in Oxidstrukturen. *Monatschefte für Chemie* **106**, 779–93.

Baur, W. H. (1970) Bond length variation and distorted coordination polyhedra in inorganic crystals. *Transactions of the American Crystallographic Association*, **6**, 129–55.

Baur, W. H. (1971) The prediction of bond length variations in silicon-oxygen bonds. *American Mineralogist*, **56**, 1573–99.

Baur, W. H. (1987) Effective ionic radii in nitrides. *Crystallography Reviews*, **1**, 59–83.

Brown, I. D. (1976) On the geometry of O-H ... O hydrogen bonds. *Acta Crystallographica*, **A32**, 24–31.

Brown, I. D. (1981) The bond-valence method: an empirical approach to chemical structure and bonding, in *Structure and Bonding in Crystals II*, (eds M. O'Keeffe and A. Navrotsky), Academic Press, New York, pp. 1–30.

Brown, I. D. and Shannon, R. D. (1973) Empirical bond-strength—bond-length curves for oxides. *Acta Crystallographica*, **A29**, 266–82.

Burdett, J. K. (1980) *Molecular Shapes*, John Wiley, New York.

Burdett, J. K. (1986) Structural–electronic relationships in the solid state, *in Molecular Structure and Energetics*, (eds A. Greenberg and J. F. Liebman), VCH Publishers, Boca Raton, pp. 209–75.

Burdett, J. K. (1987) Some structural problems examined using the method of moments. *Structure and Bonding*, **65**, 29–89.

Burdett, J. K. and Hawthorne, F. C. (1992) An orbital approach to the theory of bond-valence. *American Mineralogist*, (submitted).

Burdett, J. K. and McLarnan, T. M. (1984) An orbital interpretation of Pauling's rules. *American Mineralogist*, **69**, 601–21.

Burdett, J. K., Lee, S., and Sha, W. C. (1984) The method of moments and the energy levels of molecules and solids. *Croatia Chemica Acta*, **57**, 1193–216.

Cerny, P. and Hawthorne, F. C. (1976) Refractive indices versus alkali contents in beryl: general limitations and applications to some pegmatite types. *Canadian Mineralogist*, **14**, 491–7.

Christ, C. L. (1960) Crystal chemistry and systematic classification of hydrated borate minerals. *American Mineralogist*, **45**, 334–40.

Christ, C. L. and Clark, J. R. (1977) A crystal-chemical classification of borate structures with emphasis on hydrated borates. *Physics and Chemistry of Minerals*, **2**, 59–87.

Cromer, D. T., Kay, M. I., and Larsen, A. C. (1967) Refinement of the alum structures, II. X-ray and neutron diffraction of $NaAl(SO_4)_2{\cdot}12H_2O$. *Acta Crystallographica*, **22**, 182–7.

Ferraris, G. and Franchini-Angela, M. (1972) Survey of the geometry and environment of water molecules in crystalline hydrates studied by neutron diffraction. *Acta Crystallographica*, **B28**, 3572–83.

Fisher, D. J. (1958) Pegmatite phosphates and their problems. *American Mineralogist*, **43**, 181–207.

Gibbs, G. V. (1982) Molecules as models for bonding in silicates. *American Mineralogist*, **67**, 421–50.

Gibbs, G. V., Hamil, M. M., and Louisnathan, S. J. *et al.* (1972) Correlations between Si–O bond length, Si–O–Si angle and bond-overlap populations calculated using extended Huckel molecular orbital theory. *American Mineralogist*, **57**, 1578–613.

Hawthorne, F. C. (1979) The crystal structure of morinite. *Canadian Mineralogist*, **17**, 93–102.

Hawthorne, F. C. (1983) Graphical enumeration of polyhedral clusters. *Acta Crystallographica*, **A39**, 724–36.
Hawthorne, F. C. (1984a) The crystal structure of stenonite and the classification of the alumino-fluoride minerals. *Canadian Mineralogist*, **22**, 245–51.
Hawthorne, F. C. (1984b) The crystal structure of mandarinoite, $Fe_2^{3+}Se_3O_9 \cdot 6H_2O$. *Canadian Mineralogist*, **22**, 475–80.
Hawthorne, F. C. (1985a) Towards a structural classification of minerals: the $^{vi}M^{iv}T_2O_n$ minerals. *American Mineralogist*, **70**, 455–73.
Hawthorne, F. C. (1985b) The crystal structure of stringhamite. *Tschermaks Mineralogische und Petrographische Mitteilungen*, **34**, 15–24.
Hawthorne, F. C. (1986) Structural hierarchy in $^{vi}M_x^{iii}T_yO_z$ minerals. *Canadian Mineralogist*, **24**, 625–42.
Hawthorne, F. C. (1990) Structural hierarchy in $M^{[6]}T^{[4]}O_n$ minerals. *Zeitschrifte für Kristallographie*, **192**, 1–52.
Hawthorne, F. C. and Cerny, P. (1977) The alkali-metal positions in Cs-Li beryl. *Canadian Mineralogist*, **15**, 414–21.
Hawthorne, F. C. and Ferguson, R. B. (1975a) Anhydrous sulphates: I. Refinement of the crystal structure of celestite, with an appendix on the structure of thenardite. *Canadian Mineralogist*, **13**, 181–7.
Hawthorne, F. C. and Ferguson, R. B. (1975b) Anhydrous sulphates: II. Refinement of the crystal structure of anhydrite. *Canadian Mineralogist*, **13**, 181–7.
Hoffman, R. (1988) *Solids and Surfaces: A Chemist's view of Bonding in Extended Structures*, VCH Publishers, New York.

Liebau, F. (1985) *Structural Chemistry of Silicates*, Springer-Verlag, Berlin.

Mereiter, K. (1974) Die Kristallstruktur von Rhomboklas, $H_5O_2\{Fe[SO_4]_2 \cdot 2H_2O\}$. *Tschermaks Mineralogische und Petrographische Mitteilungen*, **21**, 216–32.
Moore, P. B. (1970a) Structural hierarchies among minerals containing octahedrally coordinating oxygen: I. Stereoisomerism among corner-sharing octahedral and tetrahedral chains. *Neues Johrbuch fur Mineralogie Monatschefte*, pp. 163–73.
Moore, P. B. (1970b) Crystal chemistry of the basic iron phosphates. *American Mineralogist*, **55**, 135–69.
Moore, P. B. (1973) Pegmatite phosphates: mineralogy and crystal chemistry. *Mineralogical, Record*, 4, 103–30.
Moore, P. B. (1974) Structural hierarchies among minerals containing octahedrally coordinating oxygen: II. Systematic retrieval and classification of octahedral edge-sharing clusters: an epistemological approach. *Neues Jahrbuch für Mineralogie Abhandlungen* **120**, 205–27.
Moore, P. B. (1975) Laueite, pseudolaueite, stewartite and metavauxite: a study in combinatorial polymorphism. *Neues Jahrbuch für Mineralogie Abhandlungen* **123**, 148–59.
Moore, P. B. (1981) Complex crystal structures related to glaserite, $K_3Na(SO_4)_2$: evidence for very dense packings among oxysalts. *Bulletin de la Societe francaise Mineralogie et Cristallographie* **104**, 536–47.
Moore, P. B. (1982) Pegmatite minerals of P(V) and B(III). *Mineralogical Association of Canada Short Course*, **8**, 267–91.
Moore, P. B. (1984) Crystallochemical aspects of the phosphate minerals, in *Phosphate Minerals*, (eds J. O. Niagru and P. B. (Moore), Springer-Verlag, Berlin, pp. 155–170.

Pabst, A. (1950) A structural classification of fluoaluminates. *American Minerulogist*, **35**, 149–65.
Pauling, L. (1929) The principles determining the structure of complex ionic crystals. *Journal of the American Chemical Society*, **51**, 1010–26.
Pauling, L. (1960) The Nature of the Chemical Bond, 3rd edn, Cornell University Press, Ithaca, New York.

Ripmeester, J. A., Ratcliffe, C. I., and Dutrizac, J. E. *et al.* (1986) Hydronium ion in the alunite-jarosite group. *Canadian Mineralogist*, **24**, 435–47.

Scordari, F. (1980) Structural considerations of some natural and artificial iron hydrated sulphates. *Mineralogical Magazine*, **43**, 669–73.
Scordari, F. (1981) Crystal chemical implications on some alkali hydrated sulphates. *Tschermaks Mineralogische und Petrographische Mitteilungen*, **28**, 207–22.
Shannon, R. D. (1975) Systematic studies of interatomic distances in oxides, in *The Physics and Chemistry of Minerals and Rocks*, (ed. R. G. J. Sterns), John Wiley & Sons, London, pp. 403–31.
Shannon, R. D. (1976) Revised effective ionic radii and systematic studies of interatomic distances in halides and chalcogenides. *Acta Crystallographica*, **A32**, 751–67.
Sutor, D. J. (1967) The crystal and molecular structure of newberyite, $MgHPO_4 \cdot 3H_2O$. *Acta Crystallographica*, **23**, 418–22.

Tossell, J. A. and Gibbs, G. V. (1977) Molecular orbital studies of geometries and spectra of minerals and inorganic compounds. *Physics and Chemistry of Minerals*, **2**, 21–57.
Trinajstic, N. (1983) *Chemical Graph Theary*, vol. I, CRC Press, Boca Raton.

Ziman, J. (1965) *Principles of the Theory of Solids*, Cambridge University Press, Cambridge.
Zoltai, T. (1960) Classification of silicates and other minerals with tetrahedral structures. *American Mineralogist*, **45**, 960–73.